Journal of Virology®

PATHOGENESIS AND IMMUNITY

Thioredoxin 2 Negatively Regulates Innate Immunity to RNA Viruses by Disrupting the Assembly of the Virus-Induced Signaling Adaptor Complex

Dan Li,[a] Wenping Yang,[a] Yi Ru,[a] Jingjing Ren,[a] Xiangtao Liu,[a] Haixue Zheng[a]

[a]State Key Laboratory of Veterinary Etiological Biology, OIE/National Foot and Mouth Disease Reference Laboratory, Lanzhou Veterinary Research Institute, Chinese Academy of Agricultural Sciences, Lanzhou, Gansu, China

ABSTRACT The virus-induced signaling adaptor (VISA) complex plays a critical role in the innate immune response to RNA viruses. However, the mechanism of VISA complex formation remains unclear. Here, we demonstrate that thioredoxin 2 (TRX2) interacts with VISA at mitochondria both *in vivo* and *in vitro*. Knockdown and knockout of TRX2 enhanced the formation of the VISA-associated complex, as well as virus-triggered activation of interferon regulatory factor 3 (IRF3) and transcription of the interferon beta 1 (*IFNB1*) gene. TRX2 inhibits the formation of VISA aggregates by repressing reactive oxygen species (ROS) production, thereby disrupting the assembly of the VISA complex. Furthermore, our data suggest that the C93 residue of TRX2 is essential for inhibition of VISA aggregation, whereas the C283 residue of VISA is required for VISA aggregation. Collectively, these findings uncover a novel mechanism of TRX2 that negatively regulates VISA complex formation.

IMPORTANCE The VISA-associated complex plays pivotal roles in inducing type I interferons (IFNs) and eliciting the innate antiviral response. Many host proteins are identified as VISA-associated-complex proteins, but how VISA complex formation is regulated by host proteins remains enigmatic. We identified the TRX2 protein as an important regulator of VISA complex formation. Knockout of TRX2 increases virus- or poly(I·C)-triggered induction of type I IFNs at the VISA level. Mechanistically, TRX2 inhibits the production of ROS at its C93 site, which impairs VISA aggregates at its C283 site, and subsequently impedes the assembly of the VISA complex. Our findings suggest that TRX2 plays an important role in the regulation of VISA complex assembly.

KEYWORDS RNA virus, ROS, TRX2, VISA

Innate immunity is the first line of defense against microbial invasion of an organism. Upon viral infection, host pattern recognition receptors (PRRs) of the innate immune system recognize invading viruses and initiate a series of signaling events leading to the production of type I interferons (IFNs) (including IFN-β and IFN-α family members) and proinflammatory cytokines (1, 2). Importantly, type I IFNs induce the expression of a series of IFN-stimulated genes (ISGs), inhibiting viral replication or causing apoptosis of infected cells and finally resulting in a cellular antiviral response (3, 4).

Viral RNA is recognized by endosomal receptor Toll-like receptor 3 (TLR3), cytosolic receptor retinoic acid-inducible gene I (RIG-I), and melanoma differentiation-associated gene 5 (MDA5). TLR3 recognizes double-stranded RNA (dsRNA) produced during viral replication and then transmits the induction signal of type I IFN through TIR domain-containing adapter-inducing IFN-β (TRIF)-dependent pathways in immune cells (5). RIG-I binds to short dsRNA and 5′-triphosphate panhandle RNA, whereas MDA5 recognizes long dsRNA (6–8). Furthermore, the C-terminal domains of RIG-I, MDA5, and

Citation Li D, Yang W, Ru Y, Ren J, Liu X, Zheng H. 2020. Thioredoxin 2 negatively regulates innate immunity to RNA viruses by disrupting the assembly of the virus-induced signaling adaptor complex. J Virol 94:e01756-19. https://doi.org/10.1128/JVI.01756-19.

Editor Bryan R. G. Williams, Hudson Institute of Medical Research

Address correspondence to Haixue Zheng, haixuezheng@163.com.

Received 11 October 2019
Accepted 18 December 2019
Accepted manuscript posted online 8 January 2020
Published 17 March 2020

RNA helicase act as cytoplasmic sensors for viral RNAs in the majority of cells (1). The ATP-dependent conformational change allows caspase recruitment domain-containing proteins (CARDs) to interact with the downstream adaptor protein virus-induced signaling adaptor (VISA) (also known as MAVS, IPS-1, and Cardif) located at the outer membrane of the mitochondria. VISA acts as a central scaffold for a virus-induced complex assembly, which triggers distinct signaling pathways and then leads to NF-κB and IRF3 activation as well as the subsequent induction of type I IFNs (9, 10).

VISA is associated with the tumor necrosis receptor-associated factor (TRAF) interaction domain of TRAF2 and TRAF6, which facilitates Lys-63-linked polyubiquitination of receptor-interacting serine/threonine protein kinase (RIP) and NF-κB essential modulator (NEMO)/IκB kinase γ (IKKγ), respectively. Afterward, the aforementioned processes result in activation of IKK and NF-κB (9, 11). VISA is also associated with TRAF3 which is essential for virus-triggered IRF3 activation and type I IFN induction (12–14). However, the molecular mechanism of VISA complex formation remains rudimentary.

Thioredoxin 2 (TRX2), encoded by a nuclear gene and localized to the mitochondria by a mitochondrial leader sequence (15), is a small redox protein containing a characteristic dithiol active site motif, Cys-Gly-Pro-Cys, which is highly conserved from bacteria to humans (16). TRX2 contains two Cys located in the catalytic sites (Cys90 and Cys93) (17). TRX2 is the main reactive oxygen species (ROS)-scavenging enzyme in mitochondria that balances ROS levels and maintains mitochondrial function in various cells (18). TRX2 can bind to apoptosis signal-regulating kinase 1 (ASK1), located in the mitochondria, and block ASK1-mediated apoptosis (17). In addition, TRX2 regulates the NF-κB signaling pathway by interacting with P65 (19). However, it is unclear whether TRX2 interacts with other mitochondrial proteins to regulate type I IFN production.

In the present study, TRX2 was identified as a novel negative regulator of virus-triggered type I IFN induction and the cellular antiviral response. We further found that TRX2 interacts with VISA and reduces the formation of VISA aggregates via C283 site-linked repression of ROS production, subsequently resulting in the disruption of VISA complex assembly. These findings provide new insights into the regulatory mechanisms of TRX2 in innate immunity.

RESULTS

TRX2 overexpression inhibits the virus-triggered IFN-β signaling pathway. TRX2 has been reported to exert opposing effects on the antiviral response, such as blocking or stimulating the tumor necrosis factor alpha (TNFα)-induced NF-κB pathway mediated by P65 (19, 20). To investigate the regulatory role of TRX2 in virus-triggered induction of type I IFNs, we performed transient-transfection and reporter assays. The results showed that TRX2 inhibited activation of the IFN-stimulated response element (ISRE), Nifty, and the IFN-β promoter approximately 1.5-fold during Sendai virus (SeV) infection (Fig. 1A to C). Consistent with this finding, TRX2 suppressed activation of the ISRE and IFN-β promoter about 2- to 3-fold during poly(I·C) treatments (Fig. 1D and E). Moreover, SeV-triggered phosphorylation of TBK1, IRF3, Iκbα, and P65, which is a hallmark of the activation of virus-triggered IFN induction pathways, was lower in TRX2-overexpressed cells than in control cells (Fig. 1F). Further experiments indicated that TRX2 overexpression inhibited SeV-triggered activation of ISRE, Nifty, and the IFN-β promoter in a dose-dependent manner (Fig. 1H to J). Real-time quantitative PCR (RT-qPCR) analysis further confirmed that the expression levels of *IFNB1*, *TNFα*, interleukin 8 (*IL-8*), *IP-10*, *ISG56*, and *IL-6* mRNAs were reduced in TRX2-overexpressed human embryonic kidney (HEK) 293T and THP-1 cells compared with that in control cells following SeV infection (Fig. 1K and M) and poly(I·C) stimulation in HEK293T cells (Fig. 1L). These results suggest that TRX2 inhibits the virus-triggered IFN-β signaling pathway and the NF-κB signaling pathway.

TRX2 knockdown potentiates virus-triggered IFN-β induction. To investigate the function of endogenous TRX2 in SeV-triggered type I IFN production, we constructed four TRX2-specific RNA interference (RNAi) plasmids, and the results showed that endogenous TRX2 expression could be reduced by transfection of those TRX2-

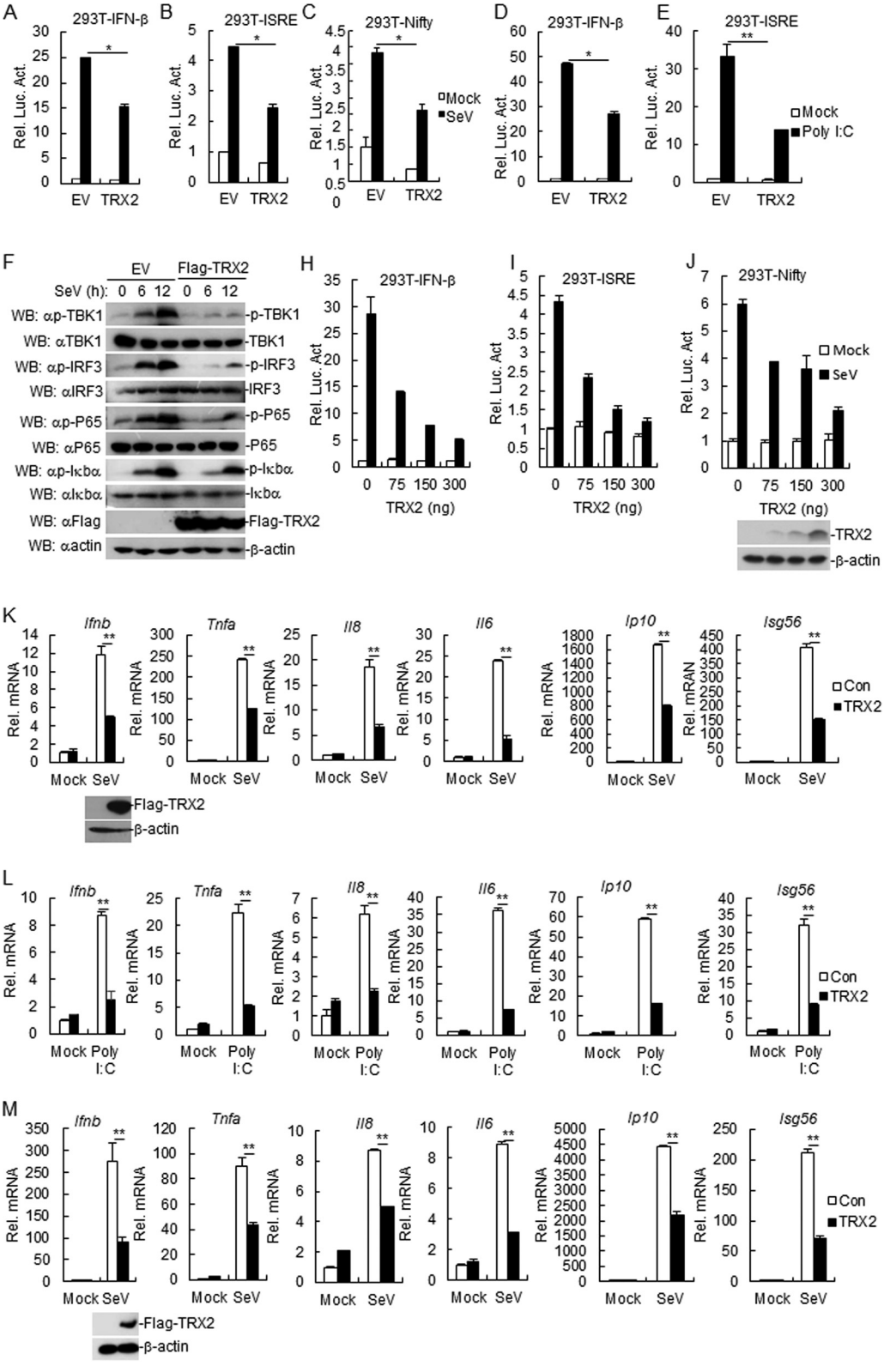

FIG 1 TRX2 inhibits virus- or poly(I·C)-triggered signaling. (A to E) Effects of TRX2 overexpression on SeV- or poly(I·C)-triggered ISRE, Nifty, and IFN-β promoter activation. HEK293T cells (1×10^5) were transfected with ISRE, IFN-β, Nifty reporter plasmids (0.1 μg), and the indicated expression plasmids (0.1 μg). At 24 h posttransfection, cells were stimulated with SeV for 12 h or with poly(I·C) (0.5 μg/ml) for 20 h before luciferase assays. Meanwhile, the unstimulated cells were served as the controls. (F) Overexpression of TRX2 inhibits SeV-induced phosphorylation of IRF3 and Iκbα. TRX2-overexpressed HEK293T cells were infected with SeV or uninfected for the indicated time points, and then cell lysates were

(Continued on next page)

specific RNAi plasmids (Fig. 2A). Reporter assays demonstrated that TRX2 knockdown potentiated activation of ISRE, Nifty, and IFN-β promoter about 1.6- to 2-fold during SeV infection (Fig. 2B to D). Likewise, TRX2 knockdown also enhanced activation of ISRE and IFN-β promoter about 1.6- to 2-fold during poly(I·C) treatments (Fig. 2E and F). Moreover, TRX2 knockdown enhanced SeV-triggered phosphorylation of TBK1, IRF3, P65, and Iκbα (Fig. 2G). RT-qPCR analysis indicated that TRX2 knockdown potentiated SeV or poly(I·C)-triggered transcription levels of endogenous *IFNB1*, *TNF*α, *IL-6*, *IL-8*, *ISG56*, and *IP-10* genes in HEK293T cells (Fig. 2H and I). Similarly, TRX2 knockdown also potentiated SeV-triggered transcription levels of the above genes in THP-1 cells (Fig. 2J). Collectively, these results suggest that knockdown of TRX2 increases virus-triggered IFN-β induction.

TRX2 knockout promotes SeV- and poly(I·C)-triggered IFN-β production. Given that TRX2 knockout in mice was reported to be embryonic lethal (21), we generated TRX2-deficient HEK293T and HeLa cells using the CRISPR-Cas9 method to further examine the roles of TRX2 in the antiviral innate immune response. Immunoblotting analysis verified that TRX2 was undetectable in TRX2 knockout HEK293T and HeLa cells (Fig. 3A and Fig. 4A). We next examined endogenous TRX2 function in the regulation of SeV- and poly(I·C)-triggered signaling. The reporter assays results showed that SeV-triggered activation of ISRE, Nifty, and IFN-β promoter in TRX2-deficient cells was about 2-fold higher than those in wild-type cells (Fig. 3A to C and Fig. 4A to C). We also found that TRX2 knockout increased the expression of IFN-β in HEK293T and HeLa cells by about 2-fold by ELISA (Fig. 3D and Fig. 4D). Similarly, activation of ISRE, Nifty, and IFN-β promoter induced by cytoplasmic poly(I·C) was increased about 1.5- to 2-fold in TRX2-deficient cells compared with wild-type cells (Fig. 3E to G and Fig 4E to G). Additionally, we found that TRX2 knockout enhanced SeV-triggered phosphorylation of TBK1, IRF3, P65, and Iκbα (Fig. 3H and Fig. 4H) RT-qPCR experiments showed that SeV-triggered transcription levels of *IFNB1*, *TNF*α, *IL-8*, and *ISG56* genes were increased in TRX2-deficient cells compared with those in wild-type cells (Fig. 3I to L and Fig. 4I to L). In line with this finding, poly(I·C) enhanced mRNA expression of *IFNB1*, *TNF*α, *IL-8,* and *ISG56* in TRX2-deficient cells compared with wild-type cells (Fig. 3M to P and Fig. 4M to P). These results suggest that TRX2 inhibits SeV-triggered activation of IRF3 and IFN-β, as well as induction of downstream cytokines and other effectors.

TRX2 knockout inhibits RNA virus replication. Given TRX2 negatively regulates RIG-I-like receptor (RLR)-mediated induction of type I IFNs, we next examined whether TRX2 affected cellular antiviral responses. The replications of SeV and vesicular stomatitis virus (VSV) were evaluated by immunoblotting analysis utilizing the antibodies against viral proteins or green fluorescent protein (GFP). We observed that expressions of the SeV protein and GFP in TRX2-deficient HEK293T (Fig. 5A) or HeLa cells (Fig. 5B) were lower than those in control cells. Besides, TRX2 knockout inhibited the mRNA level of SeV P and VSV P proteins (Fig. 5C). To further corroborate these results, VSV replication was measured by immunofluorescence microscopy and flow cytometry of VSV tagged with GFP and by plaque assays. The results showed that TRX2 knockout resulted in the decreased VSV replication, as indicated by the lessened green fluorescence immunofluorescence microscopy and flow cytometry assays (Fig. 5D) as well as about a 1.2-fold decrease in virus titers in the presence or absence of poly(I·C) (Fig. 5E)

FIG 1 Legend (Continued)
analyzed by immunoblotting with the indicated antibodies. (H to J) Dose-dependent effects of TRX2 on SeV-triggered activation of Nifty, IFN-β promoter, and ISRE. The experiments were performed as described in A to E. Expression of TRX2 was analyzed by immunoblotting. (K) Effects of TRX2 overexpression on SeV-induced transcription of downstream genes in HEK293T cells. TRX2-overexpressed HEK293T cells were infected with SeV for 12 h before RT-qPCR analysis. Expression of TRX2 was analyzed by immunoblotting. (L) Effects of TRX2 overexpression on cytoplasmic poly(I·C)-induced transcription of downstream genes. TRX2-overexpressed HEK293T cells were transfected with poly(I·C) (1 μg/ml) for 20 h before RT-qPCR analysis. (M) Effects of TRX2 overexpression on SeV-induced transcription of downstream genes in THP-1 cells. The experiments were performed as described in K. Expression of TRX2 was analyzed by immunoblotting. Data are shown as mean $\pm$ SD of three independent experiments. RT-qPCR, real-time quantitative PCR; EV, empty vector; Con, control; Luc, luciferase.

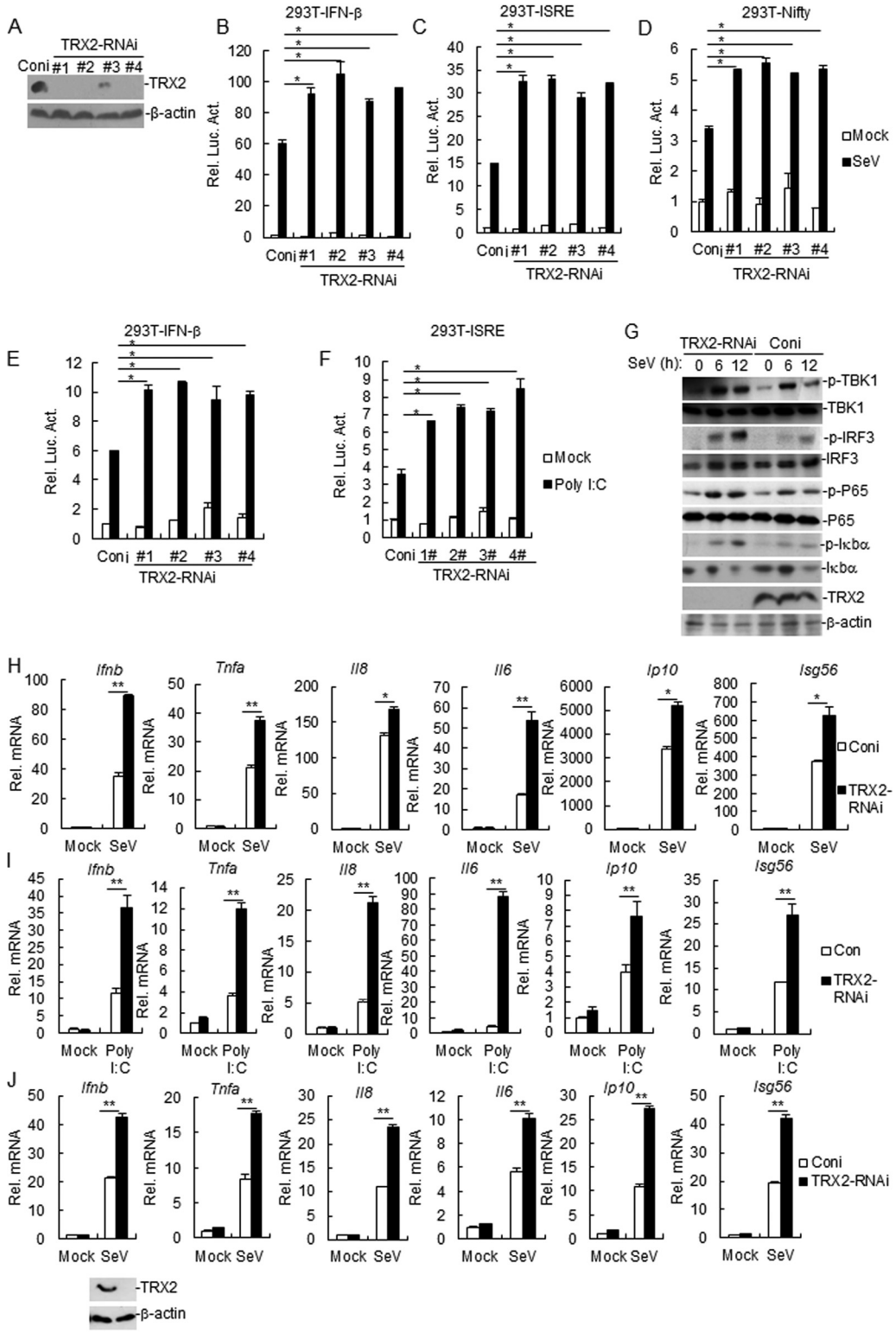

FIG 2 Effects of TRX2 knockdown on signaling triggered by various stimuli. (A) Effects of TRX2-RNAi plasmids on endogenous TRX2 expression. HEK293T cells (2×10^5) were transfected with control or indicated TRX2-RNAi plasmids (1 μg) for 24 h. Cell lysates were analyzed by immunoblotting with antibodies against TRX2 and β-actin. (B to D) Effects of TRX2-RNAi on SeV-induced activation of ISRE, Nifty, and IFN-β promoter. TRX2-knockdown HEK293T cells (1×10^5) were transfected with luciferase reporter plasmid (0.1 μg) for 24 h, and then cells were uninfected or infected with SeV for 12 h before luciferase assays. (E and F) Effects of TRX2-RNAi on poly(I·C)-induced activation of ISRE and the IFN-β promoter. TRX2-knockdown HEK293T cells (1×10^5) were transfected with luciferase reporter plasmid (0.1 μg) for 24 h, and then cells were stimulated with poly(I·C) (0.5 μg/ml) for 20 h before luciferase assays. (G) TRX2 knockdown increases SeV-induced

(Continued on next page)

in TRX2-deficient HEK293T and HeLa cells. Collectively, these observations suggest that TRX2 positively regulates RNA virus replication by inhibiting antiviral signaling.

TRX2 regulates virus-triggered signaling through interactions with VISA. Considering that the aforementioned experiments suggest that TRX2 is required for virus-triggered IRF3 and NF-κB activation, we next investigated the molecular mechanism mediated by TRX2. TRX2 overexpression inhibited IFN-β promoter activation induced by overexpression of upstream components RIG-I (CARD), MDA5, and VISA but not by downstream components TBK1, IKKε, IRF3, and IRF7 (Fig. 6A). Similarly, ISRE activation induced by VISA, but not TBK1, was inhibited by TRX2 overexpression (Fig. 6B). Hence, these data suggest that TRX2 regulates virus-induced signaling at the VISA level. Previous study has shown that TRX2 is localized in mitochondria (15). Given that VISA is a mitochondrial adaptor protein recruiting various components for assembly of a signaling complex after viral infection, we next investigated whether TRX2 is recruited to the VISA-associated complex on the mitochondria. Transient-transfection and coimmunoprecipitation (co-IP) experiments indicated that TRX2 was associated with VISA and TRAF3 but not with RIG-I, MDA5, cyclic GMP-AMP synthase (cGAS), mediator of IRF3 activation (MITA), TBK1, IKKε, IRF3, and IRF7 (Fig. 6C). Endogenous co-IP experiments further demonstrated that TRX2 was associated with VISA in HEK293T cells following SeV infection (Fig. 6D). These data suggest that TRX2 regulates virus-triggered signaling through interactions with VISA.

Effects of TRX2 on VISA-associated complex assembly. To further explore the mechanisms for the involvement of TRX2 in virus-triggered signaling, we assessed TRX2 function on the assembly of the VISA-associated complex. Interestingly, the transient-transfection and co-IP experiments showed that TRX2 overexpression impaired the association of VISA with TBK1 or TRAF6 but not with TRAF3 (Fig. 7A). Besides, we examined the role of TRX2 in the assembly of the endogenous VISA complex. Compared with the control cells, TRX2 overexpression inhibited recruitment of TBK1 and TRAF6 to the endogenous VISA complex (Fig. 7B). Consistently, TRX2 knockdown potentiated the association of VISA with TBK1 or TRAF6 (Fig. 7C). In line with this, TRX2 knockout enhanced recruitment of TBK1 and TRAF6 to the VISA complex (Fig. 7D and E). In addition, SeV infection, hydrogen peroxide (H_2O_2), and dithiothreitol (DTT) treatment did not affect the mitochondrial localization of TRX2 and VISA in HEK293T cells (Fig. 8A and B). Furthermore, mitochondrial localization of VISA in HEK293T cells was not altered by TRX2 knockout (Fig. 8C). We further found that the VISA aggregation was increased in cells treated with SeV or H_2O_2 (Fig. 8D and E). To explore the role of TRX2 in H_2O_2-mediated VISA aggregation, TRX2 knockout HEK293T cells were transfected with TRX2 or/and HA-VISA after treatment with H_2O_2. The results showed that TRX2 knockout, but not reconstitution of TRX2 in TRX2 knockout HEK293T cells, increased H_2O_2-mediated VISA aggregation (Fig. 8F). We also found that H_2O_2 increased the reconstitution of VISA aggregation in VISA knockout HEK293T cells (Fig. 8G). Collectively, these results reveal that TRX2 attenuates the recruitment of TBK1 and TRAF6 to the VISA-associated complex on the mitochondria.

TRX2 inhibits VISA aggregation. Zhao et al. have demonstrated that cytochrome *c* oxidase subunit 5B (COX5B) suppressed VISA aggregation through repressing ROS production, which balances the antiviral signaling activity (22). TRX2 plays a crucial role in defense against oxidative stress (23). To further explore the mechanisms for TRX2

FIG 2 Legend (Continued)
phosphorylation of IRF3 and Iκbα. TRX2-knockdown HEK293T cells (2×10^5) were infected with SeV or uninfected for the indicated time points, and cell lysates were analyzed by immunoblotting with the indicated antibodies. (H) Effects of TRX2-RNAi on SeV-induced transcription levels of downstream genes in HEK293T cells. TRX2-knockdown HEK293T cells were infected with SeV for the indicated time points prior to RT-qPCR analysis. (I) Effects of TRX2-RNAi on cytoplasmic poly(I·C)-induced transcription of downstream genes in HEK293T cells. TRX2-knockdown HEK293T cells were transfected with poly(I·C) (1 μg/ml) for 20 h prior to RT-qPCR analysis. (J) Effects of TRX2-RNAi on SeV-induced transcription levels of downstream genes in THP-1 cells. The experiments were performed as described in H. Expression of TRX2 was analyzed by immunoblotting. Data are shown as mean ± SD of three independent experiments. Coni, control-RNAi; RT-qPCR, real-time quantitative PCR; Luc, luciferase.

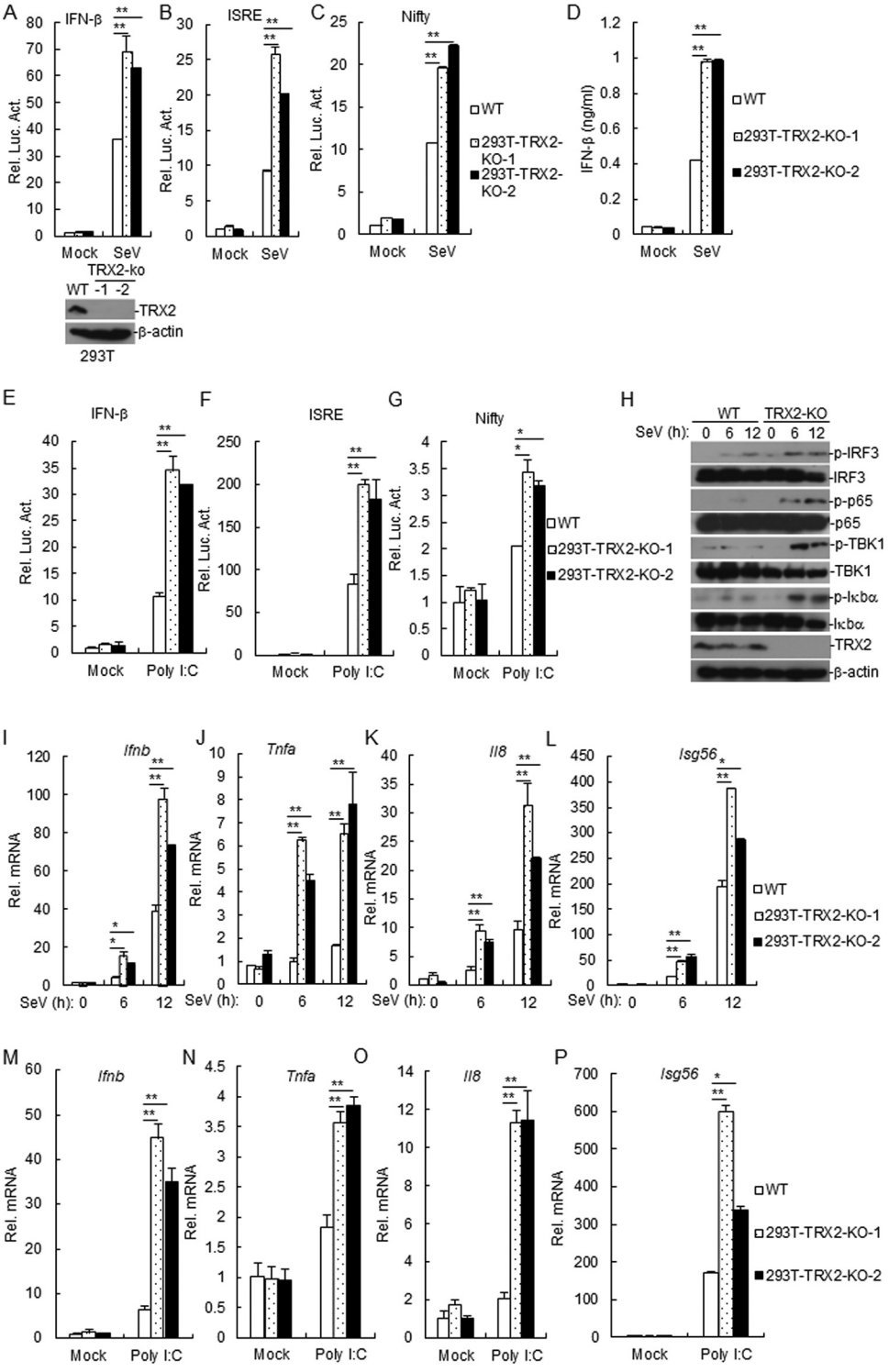

FIG 3 Effects of TRX2 knockout on virus-triggered signaling. (A to C) Effects of TRX2 knockout on SeV-triggered activation of Nifty, ISRE, and IFN-β promoter. TRX2 knockout HEK293T cells were transfected with the indicated reporter plasmids (0.1 μg). After 24 h posttransfection, cells were uninfected or infected with SeV for 12 h before luciferase assays. Expression of TRX2 was analyzed by immunoblotting. (D) Effects of TRX2 knockout on IFN-β secretion in medium supernatant. TRX2 knockout HEK293T cells (1×10^5) were infected with SeV for 18 h, and then enzyme-linked immunosorbent assay (ELISA) was performed to detect the secreted IFN-β level in the supernatant. (E to G) Effects of TRX2 knockout on cytoplasmic poly(I·C)-triggered activation of Nifty, ISRE, and IFN-β promoter. TRX2 knockout cells were transfected with the indicated reporter plasmids (0.1 μg) for 24 h, and then cells were retransfected with poly(I·C) (0.5 μg/ml) for 20 h prior to luciferase assays. (H) TRX2 knockout increases SeV-induced phosphorylation of IRF3 and Iκbα. TRX2 knockout cells were infected with SeV or uninfected for the indicated time

(Continued on next page)

involvement in virus-triggered signaling, we examined the roles of TRX2 in VISA aggregation. TRX2 overexpression reduced VISA aggregation (Fig. 9A), whereas TRX2 knockout increased VISA aggregation both in HEK293T and HeLa cells after SeV infection (Fig. 9B). A previous study reported that ROS could enhance disulfide bond formation (24). Therefore, we investigated if the disulfide bond of VISA influences VISA aggregation. We first identified 10 conserved cysteine residues (C13, C20, C33, C46, C79, C133, C283, C435, C452, and C508) of VISA by sequence analysis and then constructed a series of VISA mutants through mutating those cysteine residues to serine. As shown in Fig. 9D, mutation of C283 to serine reduced VISA aggregation. We further found that TRX2 knockout and reconstitution of TRX2C93S and TRX2C90/93S, but not reconstitution of TRX2 and TRX2C90S in TRX2 knockout HEK293T cells, increased VISA-mediated activation of the IFN-β promoter (Fig. 9E). In reporter assays, VISA C283S inhibited VISA-triggered activation of the IFN-β promoter and ISRE, whereas TRX2 did not affect VISA C283S-triggered activation of the IFN-β promoter and ISRE (Fig. 9F and G). In addition, we found that TRX2 did not affect the expression of VISA and its mutants (Fig. 9H). Further experiments indicated that TRX2-inactivated mutants (individual C93 mutation or double C90 and C93 mutation) exhibited no effect on VISA aggregation (Fig. 9I). Collectively, these results suggest that the TRX2 C93 residue is essential for inhibition of VISA aggregation, whereas the VISA C283 residue is required for its aggregation.

TRX2 inhibits VISA signaling via repressing ROS production. We next determined the molecular mechanism underlying the action of TRX2 in the VISA-mediated antiviral pathway. Previous studies have revealed that VISA overexpression increased ROS production (22). To assess the effect of VISA, VISAC283S, TRX2, TRX1, and mito-TEMPO on ROS production, fluorescence-activated cell sorter (FACS) analysis was conducted after transfection of empty vector, VISA, TRX2, TRX1, and VISAC283S plasmids or treated with mito-TEMPO. VISA, but not VISAC283S transfection, led to the upregulation of cellular and mitochondrial ROS production, whereas TRX2 and mito-TEMPO inhibited cellular and mitochondrial ROS production (Fig. 10A). Importantly, TRX1 inhibited cellular ROS production but not mitochondrial ROS production (Fig. 10A). To explore the role of TRX2 mutants in VISA aggregation, reconstitutions of TRX2 mutants in TRX2 knockout HEK293T cells were transfected with hemagglutinin (HA)-VISA after treatment or no treatment with mito-TEMPO. The results showed that reconstitution of TRX2 and TRX2C90S, but not TRX2C93S in TRX2 knockout HEK293T cells, inhibited VISA aggregation. Moreover, mito-TEMPO reversed the effect of TRXC93S on VISA aggregation (Fig. 10B). Previous studies have unraveled that TRX2 knockout resulted in the dysfunction of mitochondria in cultured cells and an increase of ROS production, suggesting that TRX2 has a critical role in mitochondrial electron transport and oxygen tolerance (18). We then identified whether TRX2 and its inactivated mutants (TRX2C90S and TRX2C93S) had an impact on ROS production induced by VISA or VISAC283S. The results suggest that overexpression of TRX2 and TRX2C90S, but not TRX2C93S, inhibited the ROS increase induced by VISA (Fig. 10C). In contrast, the VISAC283S mutant did not affect the ROS decrease by TRX2 or TRX2C90S (Fig. 10C). In addition, coexpression of VISAC283S and TRX2C93S did not affect ROS production compared with the controls (Fig. 10C). To further investigate the effects of TRX2 on the ROS increase induced by VISA, we determined whether TRX2 knockout promoted VISA-induced enhanced ROS production. The results indicated that TRX2-deficient HEK293T cells or HeLa cells potentiated ROS production induced by VISA, but not VISAC283S (Fig. 10D and E).

FIG 3 Legend (Continued)
points; subsequently, cell lysates were analyzed by immunoblotting with the indicated antibodies. (I to L) Effects of TRX2 knockout on SeV-induced transcription levels of downstream genes. TRX2 knockout HEK293T cells were infected with SeV for the indicated time points prior to RT-qPCR analysis. (M to P) Effects of TRX2 knockout on cytoplasmic poly(I·C)-induced transcription levels of downstream genes. TRX2 knockout HEK293T cells were transfected with poly(I·C) (1 μg/ml) for 20 h prior to RT-qPCR analysis. Data are shown as mean $\pm$ SD of three independent experiments. KO, knockout; WT, wild type; RT-qPCR, real-time quantitative PCR; Luc, luciferase.

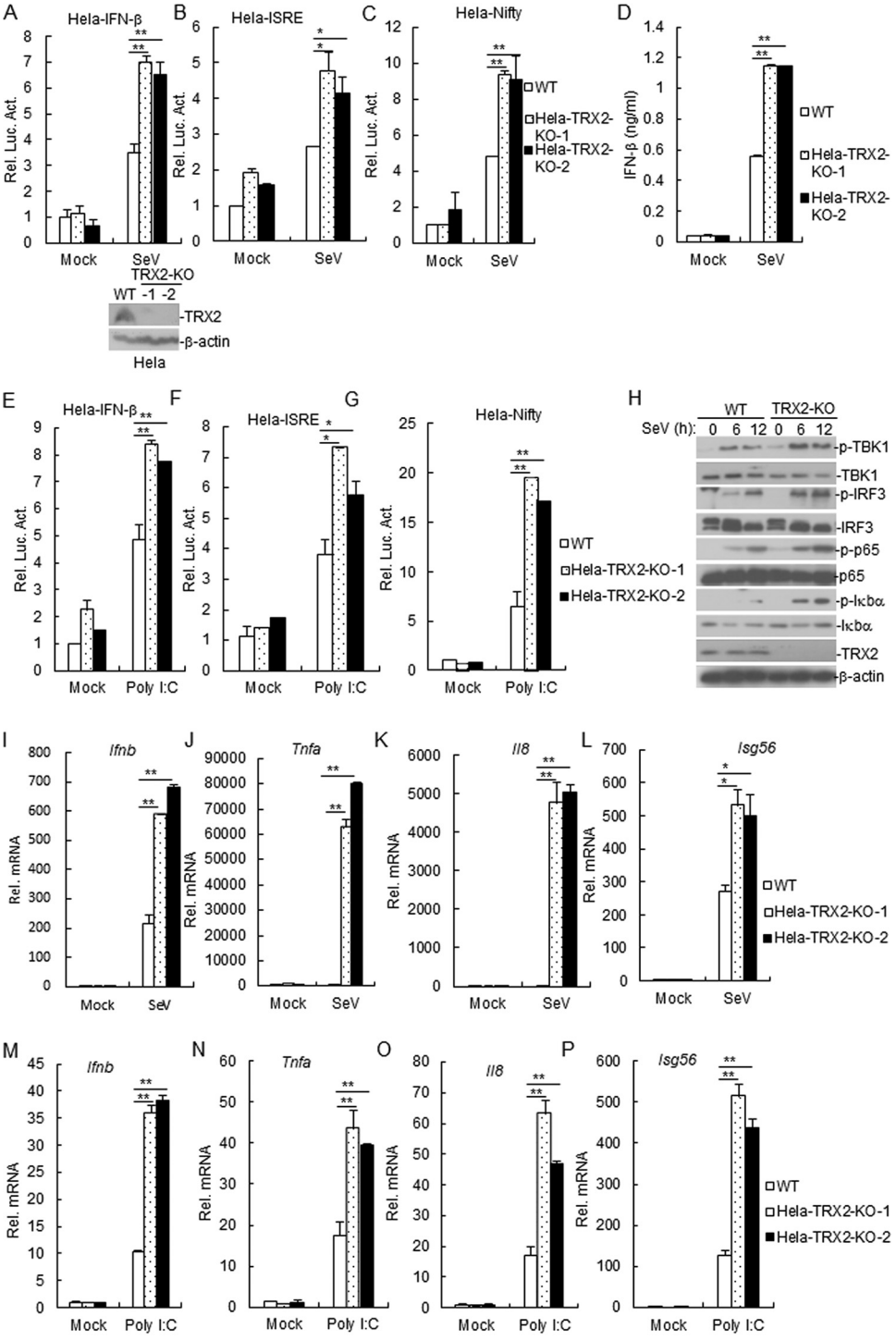

FIG 4 Effects of TRX2 knockout on virus-triggered signaling. (A to C) Effects of TRX2 knockout on SeV-triggered activation of Nifty, ISRE, and IFN-β promoter. TRX2 knockout HeLa cells were transfected with the indicated reporter plasmids (0.1 μg). After 24 h posttransfection, cells were uninfected or infected with SeV for 12 h before luciferase assays. Expression of TRX2 was analyzed by immunoblotting. (D) Effects of TRX2 knockout on IFN-β secretion in medium supernatant. TRX2 knockout HeLa cells (1×10^5) were infected with SeV for 18 h, and then ELISA was performed to detect the secreted IFN-β level in the supernatant. (E to G) Effects of TRX2 knockout on cytoplasmic poly(I·C)-triggered activation of Nifty, ISRE, and IFN-β promoter. TRX2 knockout cells were transfected with Nifty, ISRE, or IFN-b promoter reporter plasmids (0.1 μg). After 24 h posttransfection, cells were retransfected with buffer or poly(I·C) (0.5 μg/ml) for 20 h prior to luciferase assays. (H) Knockout of TRX2 increases SeV-induced phosphorylation of IRF3 and Iκbα. TRX2 knockout cells were infected with SeV or were uninfected for the indicated time points. Cell lysates were analyzed by immunoblotting with the indicated antibodies. (I to L) Effects of TRX2 knockout on SeV-induced transcription of downstream genes. TRX2 knockout HeLa cells were infected with SeV for

(Continued on next page)

Taken together, our data indicate that TRX2 negatively regulates VISA signaling through repressing ROS production.

The TRX2 C93 site and VISA C283 site play vital roles in the assembly of the VISA complex. To identify whether the active sites of TRX2 affect the assembly of the VISA complex, the transient-transfection and co-IP experiments were performed. The TRX2 C90S mutant disrupted the assembly of VISA-TBK1 complex, whereas TRX2 C93S and TRX2 C90/93S mutants lost this ability (Fig. 11A to C). Similarly, the TRX2 C90S mutant, but not TRX2 C93S and TRX2 C90/93S mutants, impeded the assembly of the VISA-TRAF6 complex (Fig. 11D to F). We further interrogated whether the VISA C283 site is a key determinant of TRX2-mediated formation of the VISA complex via the co-IP experiment. Interestingly, we observed that TRX2 overexpression did not affect the assembly of the VISA C283S-TBK1/TRAF6 complex (Fig. 11G and H). Taken together, these data indicate that the TRX2 C93 site and VISA C283 site play pivotal roles in the assembly of the VISA complex.

DISCUSSION

Previous studies have revealed that the mitochondrial outer membrane protein VISA plays a central role in an assembly complex mediating IRF3 and NF-κB activation in response to viral infection (9, 25–27). Several lines of evidence suggest that some host proteins act as a VISA-associated component required for virus-triggered activation of IRF3 and NF-κB as well as induction of IFN-β, such as WD repeat domain 5 (WDR5) (28), ECSIT signaling integrator (ECSIT) (29), and ring finger protein 5 (RNF5) (30). In the present study, we showed that TRX2 inhibited virus-triggered activation of IRF3 and NF-κB as well as IFN-β induction through disrupting the formation of the VISA-associated signaling complex.

VISA plays the central role in the RLR-mediated antivirus signaling pathway (31). VISA is associated with TRAF3 and TRAF6 through its TRAF-interacting motifs to activate IRF3 and NF-κB, respectively (9, 12, 27). Nevertheless, TRAF6 plays an important role in the activation of IRF3 and NF-κB, whereas TRAF3 is dispensable for TBK1 and IRF3 activation (32, 33). In addition, G patch domain-containing protein 3 (GPATCH3) has been identified to negatively regulate RLR-mediated activation of IRF3 and NF-κB through interrupting the binding of VISA to TRAF6 but not TRAF3 (34). Consistent with this, we identified TRX2 as a negative regulator of RLR-mediated activation of IRF3 and NF-κB by interrupting the binding of VISA to TRAF6 but not TRAF3. Additionally, UBX domain protein 1 (UBXN1) negatively regulates VISA function by competing for the TRAF-binding motifs of VISA to block recruitment of TRAF3 and TRAF6 (35). The GPATCH3 disruption assembly of the VISA-complex was dependent on the membrane localization of VISA to inhibit RLR-mediated activation of both IRF3 and NF-κB (34). The mechanism of TRX2-mediated assembly of the VISA complex is different from UBXN1 and GPATCH3. Here, our findings demonstrated that TRX2 interacted with VISA and negatively regulates the function of VISA by impairing VISA aggregates.

The TRAF3 sequence was highly homologous to TRAF6, all of which contain a conserved TRAF domain, a TRAF-C domain, an N-terminal RING domain, and zinc finger motifs (36, 37). Notably, both TRAF3 and TRAF6 were constitutively associated with VISA (28). However, several divergences have been reported about the function of TRAF3 and TRAF6. For instance, the TRAF6-dependent pathway targets mitogen-activated protein kinases (MAPKs) and IKK, resulting in the activation of transcription factors, such as AP-1 and NF-κB, that participate in the induction of proinflammatory cytokines. However, TRAF3 is dispensable for MAPK and IKK activation or production of proinflammatory cytokines (14). In this study, we found that TRX2 negatively regulated type

FIG 4 Legend (Continued)
the indicated time points prior to RT-qPCR analysis. (M to P) Effects of TRX2 knockout on cytoplasmic poly(I·C)-induced transcription of downstream genes. TRX2 knockout HeLa cells were transfected with poly(I·C) (1 μg/ml) for 20 h prior to RT-qPCR analysis. Data are shown as mean $\pm$ SD of three independent experiments. RT-qPCR, real-time quantitative PCR; KO, knockout; WT, wild type.

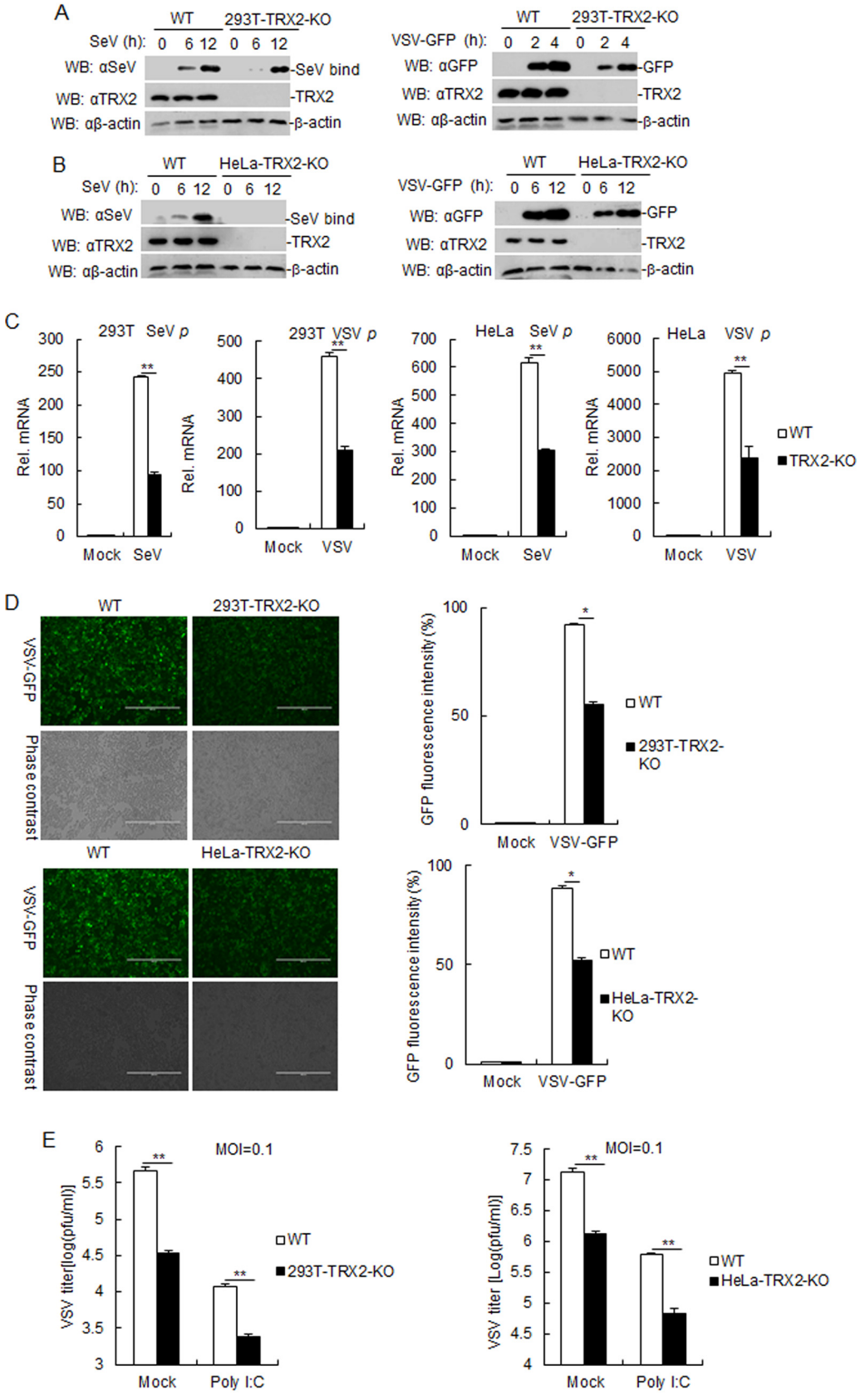

FIG 5 TRX2 knockout negatively regulates the cellular antiviral response. TRX2-deficient HEK293T cells (A) or HeLa cells (B) were infected with SeV or VSV-GFP (MOI, 0.1) for the indicated time points, and then the cell lysates were analyzed by immunoblotting with the antibodies against SeV protein, GFP, or β-actin protein. (C) Effects of TRX2 deficiency on SeV and

(Continued on next page)

I IFNs by disrupting the VISA-TBK1 interaction and VISA-TRAF6 interaction but not the VISA-TRAF3 interaction, supporting the view that TRAF3 and TRAF6 really display a different function.

ROS have emerged as important players in regulating innate immunity, particularly in the antiviral signaling pathway (38, 39). It has been demonstrated that ROS are essential for effective activation of signaling pathways, thereby leading to a successful innate immune response against herpes simplex virus (HSV) infection (39). Previous studies have revealed that NADPH oxidase 2 (NOX2) and ROS are critical for the ability of the host cell to trigger an efficient RIG-I-mediated IRF3 activation and downstream antiviral genes through regulation of VISA expression (38). In addition, COX5B down-regulated VISA signaling by repressing ROS production and negatively regulated cellular antivirus response (22). Here, we found that TRX2 inhibited the VISA-mediated signaling pathway by impairing ROS production, which is consistent with the above views; however, we found that ROS affected VISA aggregation and resulted in the disruption of the VISA complex formation.

C90 and C93 sites of TRX2 have an important role in TRX2 function (23). It has been demonstrated that the reaction mechanism of TRX2 involves an initial C90 thiolate attack on target disulfides followed by a reduction of the intermediate TRX2 target protein disulfide by C93 (23). In addition, the C90 site of TRX2, but not the C93 site, is critical for ASK1 binding (17), suggesting that C90 and C93 sites of TRX2 exhibit different functions. In this study, we found that the TRX2 C93 site, but not C90, was involved in inhibiting the VISA-mediated signaling pathway, indicating that TRX2 C93S and TRX2 C90S have distinct functions in inhibiting the VISA-mediated signaling pathway. However, the mechanisms that display the different functions at the C90 and C93 sites of TRX2 need to be elucidated in the future.

In conclusion, we propose a working model of TRX2-mediated regulation of VISA-mediated innate antiviral responses to RNA viruses. In resting cells, TRX2 constitutively interacts with VISA in mitochondria. TRX2 inhibited the VISA-triggered signaling pathway at the VISA C283 site by repressing ROS production, which disrupts the VISA-TBK1 and VISA-TRAF6 interaction. Overall, our results provide important insights into the molecular mechanisms of VISA complex formation.

MATERIALS AND METHODS

Reagents, antibodies, and cells. Antibodies against Myc, TRX2, VISA, p-P65, P65, p-IRF3, IRF3, p-Iκbα, and Iκbα were all purchased from Cell Signaling; AIF antibody (mitochondrial marker) was from Santa Cruz Biotechnology; anti-Flag, anti-HA, and anti-β-actin were from Sigma; horseradish peroxidase (HRP)-conjugated anti-mouse IgG and anti-rabbit IgG were from Thermo; and HRP-conjugated anti-goat IgG was from Zhong Shan Jin Qiao. SeV and VSV-GFP were previously described (40, 41). VISA knockout HEK293T cells were provided by the indicated investigators (Hong-Bing Shu, Wuhan University). Rabbit polyclonal anti-SeV was as previously described (42). HEK293T cells, THP-1 cells, and HeLa cells were cultivated as previously described (9, 43).

Plasmids. Luciferase reporter plasmids under the control of Nifty (a NF-κB reporter), ISRE, and IFN-β promoter as well as mammalian expression plasmids encoding RIG-I (CARD), MDA5, VISA, TBK1, IKKε, TRAF6, IRF3, and IRF7 were generated as previously described (44). Cytomegalovirus (CMV) promoter-based mammalian expression plasmids encoding Myc- or Flag-tagged TRX2 and Flag-tagged TRX1 were constructed by standard molecular biology techniques. Mammalian expression plasmids for VISA or TRX2 mutants were generated via the standard mutagenesis method.

Reporter assays. The corresponding plasmids were transfected into HEK293T cells (1×10^5) by standard calcium phosphate precipitation for 12 h. To normalize the transfection efficiency, 0.01 μg of pRL-TK (Renilla luciferase) reporter plasmid was added to each transfection. Luciferase reporter assays

FIG 5 Legend (Continued)
VSV infection. TRX2-deficient HEK293T cells were infected with SeV for 12 h or VSV-GFP (MOI, 0.1) for 4 h. Similarly, TRX2-deficient HeLa cells were infected with SeV or VSV-GFP (MOI, 0.1) for 12 h. The uninfected cells were regarded as the controls. The mRNA levels of SeV P and VSV P proteins were determined by RT-qPCR. (D) TRX2-deficient HEK293T cells (left) or HeLa cells (right) were infected with VSV-GFP (MOI, 0.1) for 4 h (HEK293T) or 12 h (HeLa). Cell images were captured by fluorescence microscopy. In addition, the GFP fluorescence levels in VSV-GFP-infected cells were analyzed by flow cytometry. (E) Effects of TRX2-deficient HEK293T cells (left) or HeLa cells (right) on VSV titer. TRX2-deficient HEK293T or HeLa cells were transfected with 1 μg/ml poly(I·C) for 16 h and then infected with VSV-GFP (MOI, 0.1) for 18 h. Supernatants were analyzed for evaluating VSV production by standard plaque assays. Data are shown as mean ± SD of three independent experiments. KO, knockout; WT, wild type; RT-qPCR, real-time quantitative PCR.

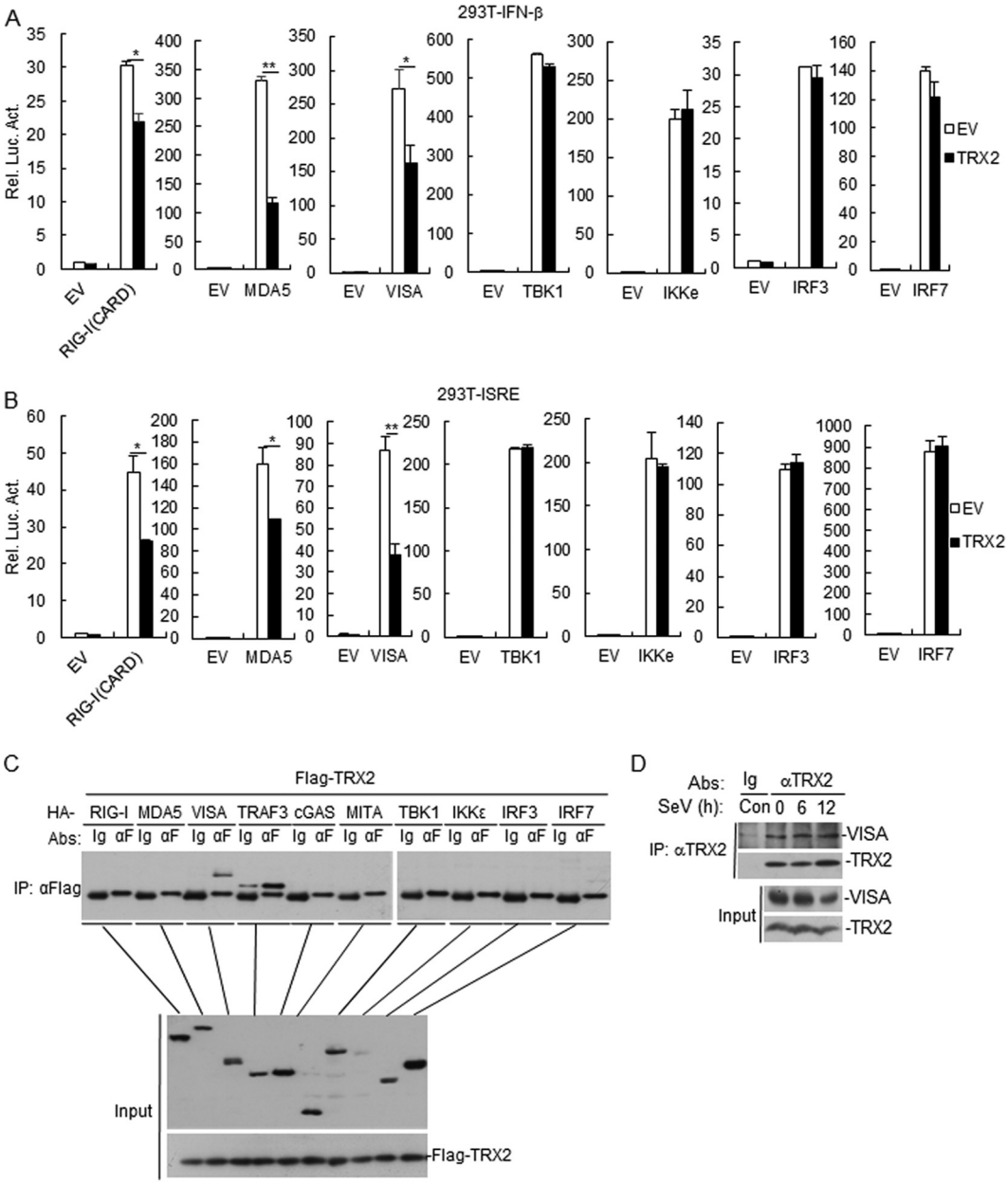

FIG 6 TRX2 interacts with VISA and targets upstream of VISA. (A and B) Effects of TRX2 on the activation of IFN-β promoter and ISRE. HEK293T cells (1×10^5) were transfected with IFN-β promoter, ISRE reporter plasmids (0.1 μg), and the indicated expression plasmids (0.1 μg each). Luciferase assays were performed at 24 h posttransfection. (C) TRX2 interacts with VISA. HEK293T cells were transfected with the indicated plasmids for 24 h before co-IP and immunoblotting analyses. The sample quantity was too large, so different protein gels were used for detecting IP samples. (D) Endogenous associations between TRX2 and VISA. HEK293T cells were uninfected or infected with SeV for the indicated time points prior to co-IP and immunoblotting analyses. Data are shown as mean ± SD of three independent experiments. Co-IP, Coimmunoprecipitation; EV, empty vector; F, Flag tag; αF, anti-Flag; Luc, luciferase.

were carried out utilizing a dual-specific luciferase assay kit (Promega). Firefly luciferase activities were measured and normalized based on Renilla luciferase activities. Here, all reporter assays were repeated in triplicate.

Semidenaturing detergent agarose gel electrophoresis. Semidenaturing detergent agarose gel electrophoresis (SDD-AGE) was implemented according to a previous protocol (45, 46). Briefly, cells were homogenized in a buffer (10 mM Tris-HCl [pH 7.5], 10 mM KCl, 1.5 mM $MgCl_2$, 0.25 M D-mannitol, and Roche EDTA-free protease inhibitor cocktail) by repeated douncing. Crude mitochondria (P5) were resuspended and loaded onto a vertical 1.5% agarose gel after differential centrifugation and purification. Ultimately, electrophoresis and immunoblotting were conducted as previously described (45).

Co-IP and immunoblotting analysis. For transient-transfection and exogenous co-IP experiments, HEK293T cells (2×10^6) were transfected with the indicated plasmids for 24 h. Then, cells were lysed in

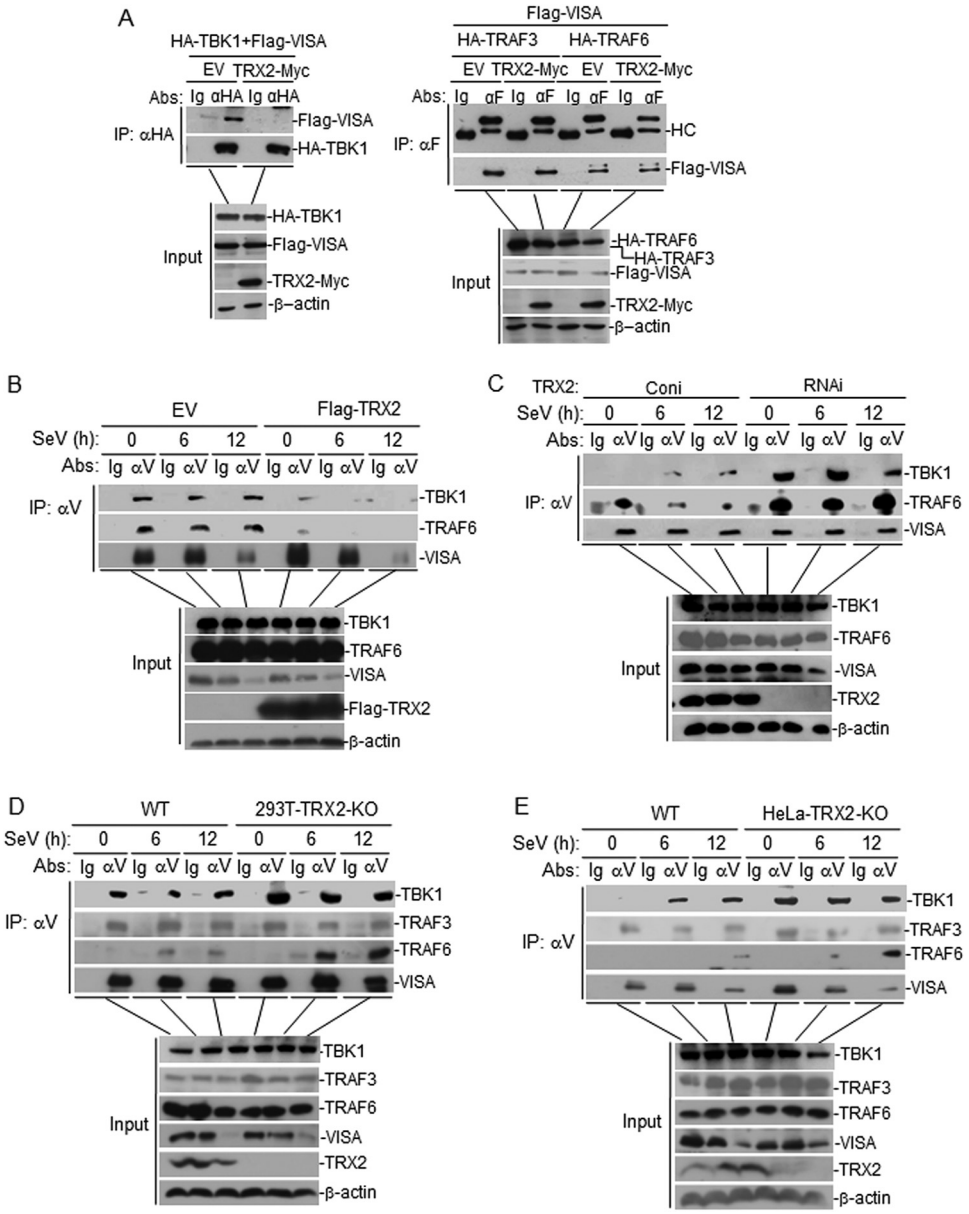

FIG 7 Effects of TRX2 on assembly of the VISA-associated complex. (A) Overexpression of TRX2 disrupts the VISA-associated complex assembly. HEK293T cells (2×10^6) were transfected with the indicated plasmids (5 μg each). Co-IP and immunoblotting analyses were conducted with the indicated antibodies. (B) TRX2-overexpressed HEK293T cells were infected with SeV for indicated time points before co-IP and immunoblotting analyses. (C) Knockdown of TRX2 enhanced the VISA-associated complex assembly. The experiments were performed as described in B. (D and E) TRX2 knockout enhanced assembly of the VISA-associated complex in HEK293T and HeLa cells. TRX2 knockout cells were infected with SeV for the indicated time points before co-IP and immunoblotting analyses. Co-IP, coimmunoprecipitation; EV, empty vector; αF, anti-Flag; αV, anti-VISA, Coni, control RNAi; WT, wild type; KO, knockout; HC, heavy chain.

1 ml of lysis buffer (15 mM Tris [pH 7.5], 150 mM NaCl, 1% Triton, 25 mM KCl, 2 mM EGTA, 2 mM EDTA, 0.1 mM dithiothreitol, 0.5% Triton X-100, 10 μg/ml aprotinin, 10 μg/ml leupeptin, and 0.5 mM phenylmethylsulfonyl fluoride). For each immunoprecipitation, a 0.4-μl aliquot of lysate was incubated with 0.2 μg of the indicated monoclonal antibody or control mouse IgG and 20 μl of GammaBind G Plus Sepharose (Amersham Biosciences) for 2 h at 4°C. The Sepharose beads were washed three times with 1 ml of lysis buffer containing 0.5 M NaCl. The precipitates were analyzed as previously described (47, 48).

For endogenous co-IP experiments, cells were uninfected or infected with SeV for the indicated time points. Cells were then lysed in 5 ml of lysis buffer, and the lysate was incubated with 1 μg of the indicated antiserum or preimmune control serum. The subsequent procedures were carried out as aforementioned.

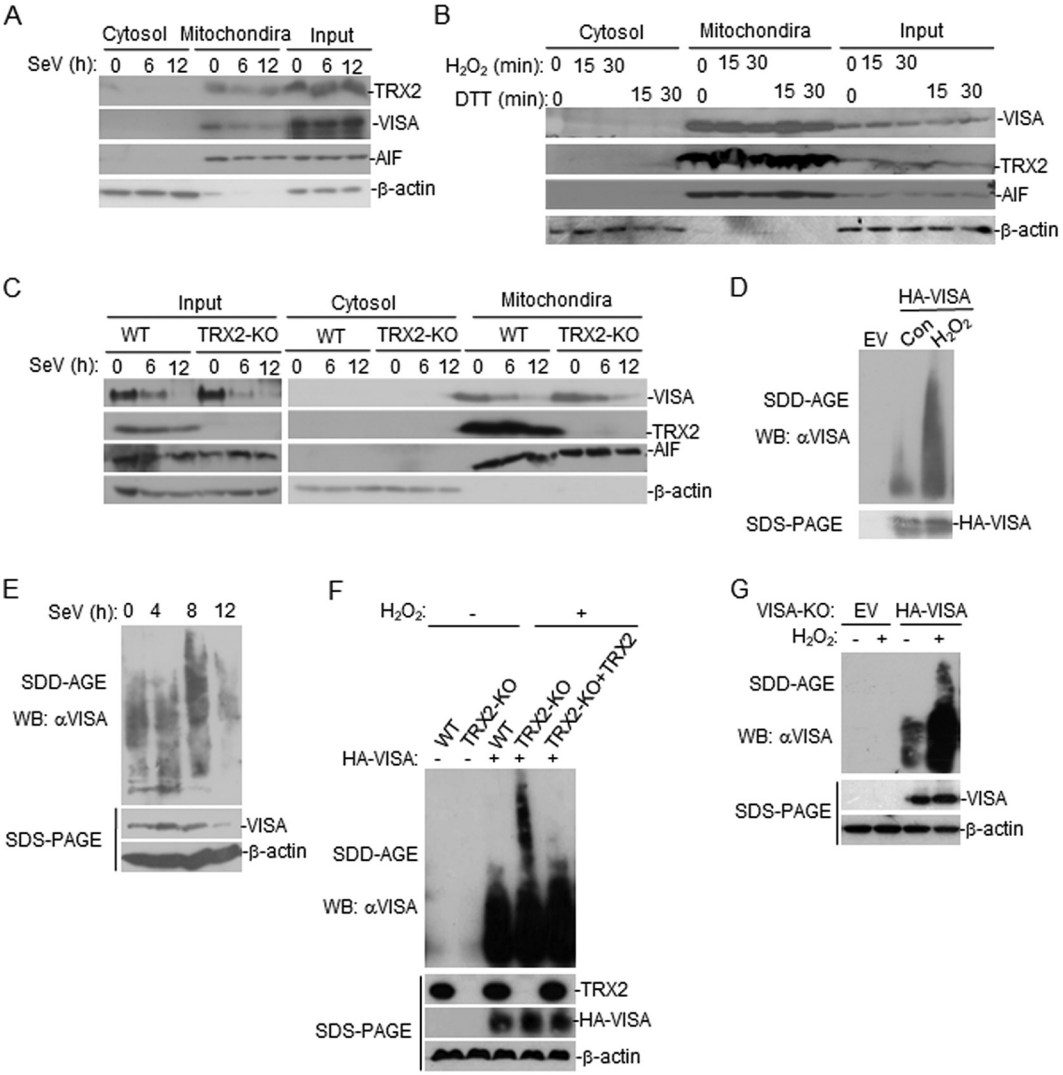

FIG 8 TRX2 and VISA are localized at mitochondria. (A) Cell fractionation and immunoblotting analysis of the subcellular fractions were conducted after viral infection. HEK293T cells were infected with SeV for the indicated time points or uninfected. Cell fractionations were performed and then the fractions were analyzed in equal volume by immunoblotting with the indicated antibodies. (B) Cell fractionation and immunoblotting analysis of the subcellular fractions were performed after treatment with H_2O_2 and DTT. HEK293T cells were treated with H_2O_2 (10 mM) and DTT (5 mM) for the indicated time points or untreated. Cell fractionation was collected, and then the fractions were analyzed in equal volume by immunoblotting with the indicated antibodies. (C) TRX2 knockout did not affect the mitochondrial location of VISA in HEK293T cells. TRX2 knockout HEK293T cells were infected with SeV for the indicated time points or uninfected. Cell fractionation was collected, and then the fractions were analyzed in equal volume by immunoblotting with the indicated antibodies. (D) H_2O_2 treatment increased the formation of VISA aggregation. Crude mitochondrial extracts were isolated from HEK293T cells treated for 30 min with H_2O_2 (10 mM), and then aliquots of the extracts were analyzed by SDD-AGE and SDS-PAGE. (E) Viral infection increased the formation of VISA aggregation. Crude mitochondrial extracts were isolated from HEK293T cells infected with SeV for the indicated time points, and then aliquots of the extracts were analyzed by SDD-AGE and SDS-PAGE. (F) TRX2 knockout increased H_2O_2-mediated VISA aggregation. TRX2 knockout or reconstitution of TRX2 in TRX2 knockout HEK293T cells were transfected with HA-VISA for 24 h after treating for 30 min with H_2O_2 (10 mM), and then the cell extracts were analyzed by SDD-AGE and SDS-PAGE. (G) H_2O_2 increased VISA aggregation. The experiments were performed as described in F. Con, control; EV, empty vector. KO, knockout; WT, wild type.

ROS evaluation and flow cytometric analysis. Cells were stained with MitoSOX at a final concentration of 5 μm for 30 min at 37°C in the dark to measure the mitochondrial ROS superoxide content. Similarly, cells were stained with 2.5 μm of CM-H2DCFDA (DCF; Molecular Probes, Invitrogen) for 15 min at 37°C in the dark to measure the total cellular ROS content. Cells were then washed with PBS solution and resuspended in phosphate-buffered saline (PBS) solution containing 1% fetal bovine serum (FBS) for FACS analysis. All data were analyzed with Cell Quest software.

RT-qPCR. Total RNA was isolated from HEK293T cells utilizing the TRIzol reagent (Invitrogen) according to the manufacturer's instructions. Then, RT-qPCR analysis was performed to measure expressions of *IFNB1*, *TNFα*, *IL-8*, *IL-6*, *IP-10*, *ISG56*, *SeV P*, *VSV P*, and *GAPDH* genes with the primers listed in Table 1.

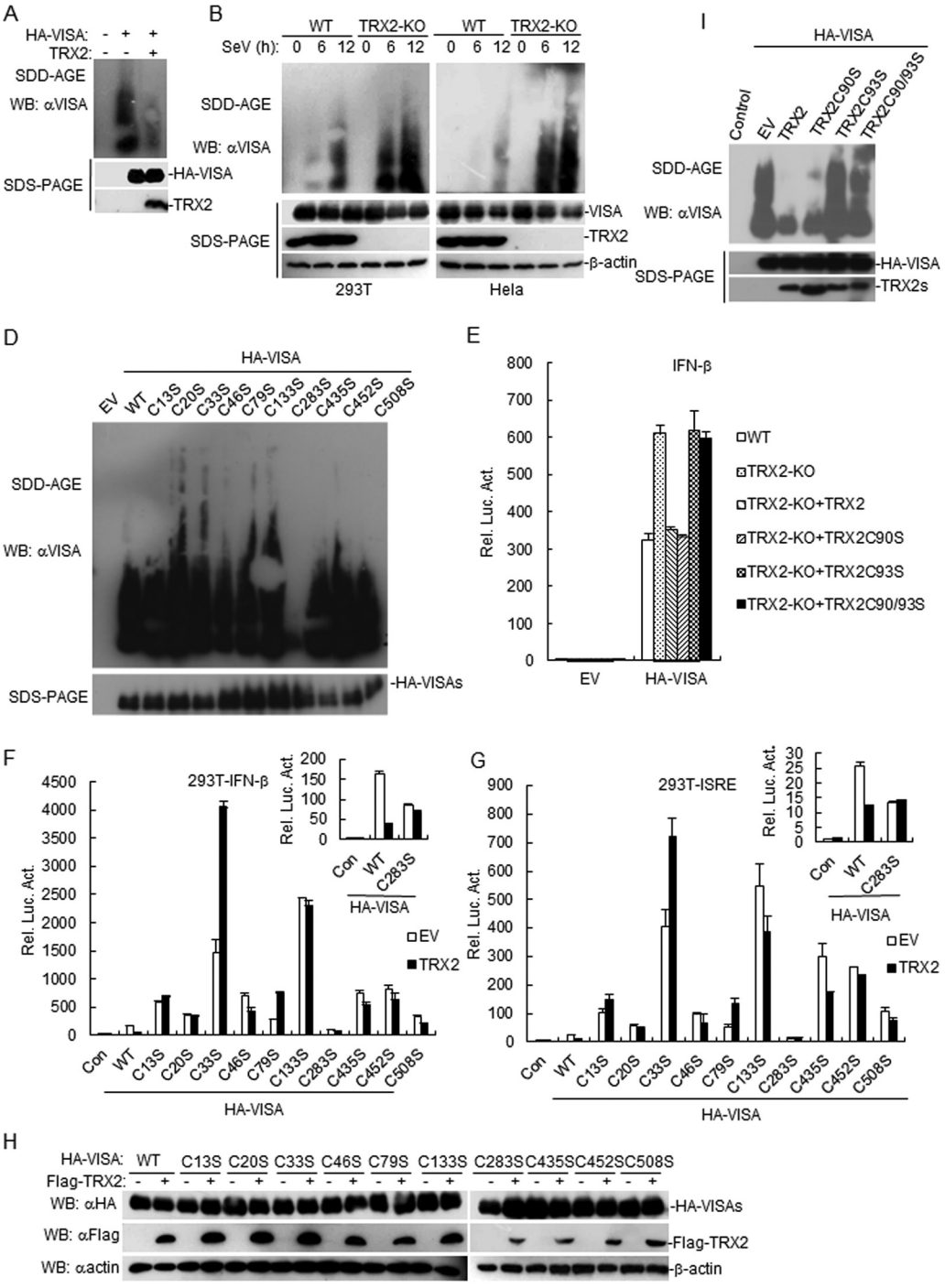

FIG 9 TRX2 suppresses VISA aggregation. (A) Overexpression of TRX2 inhibited VISA aggregation. HEK293T cells were transfected with the indicated plasmids for 24 h. Thereafter, crude mitochondrial extracts were isolated, and then aliquots of the extracts were subjected to SDD-AGE and SDS-PAGE assays utilizing the indicated antibodies. (B and C) Knockout of TRX2 promoted VISA aggregation in HEK293T and HeLa cells. TRX2-deficient HEK293T and HeLa cells were uninfected or infected with SeV for the indicated time points. Crude mitochondrial extracts were prepared, and SDD-AGE and SDS-PAGE assays were performed using VISA or TRX2 antibodies. (D) Effects of VISA and its mutants on VISA aggregation. The experiments were performed as described in A. (E) Effects of TRX2 mutants on VISA triggered the activation of the IFN-β promoter. TRX2-knockout HEK293T cells (1×10^5) were transfected with the indicated reporters (0.1 μg) and plasmids encoding VISA (0.1 μg) for 24 h before reporter assays. (F and G) Effects of VISA and its mutants on the activation of IFN-β promoter and ISRE. The experiments were performed as described in E. (H) Effects of TRX2 on the expression of VISA and its mutants. HEK293T cells were transfected with the indicated plasmids (0.4 μg) for 24 h before immunoblotting analysis. (I) Effects of TRX2 and its mutants on VISA aggregation. The experiments were performed as described in A. Data are shown as mean $\pm$ SD of three independent experiments. WT, wild type; KO, knockout; EV, empty vector; Luc, luciferase; Con, control.

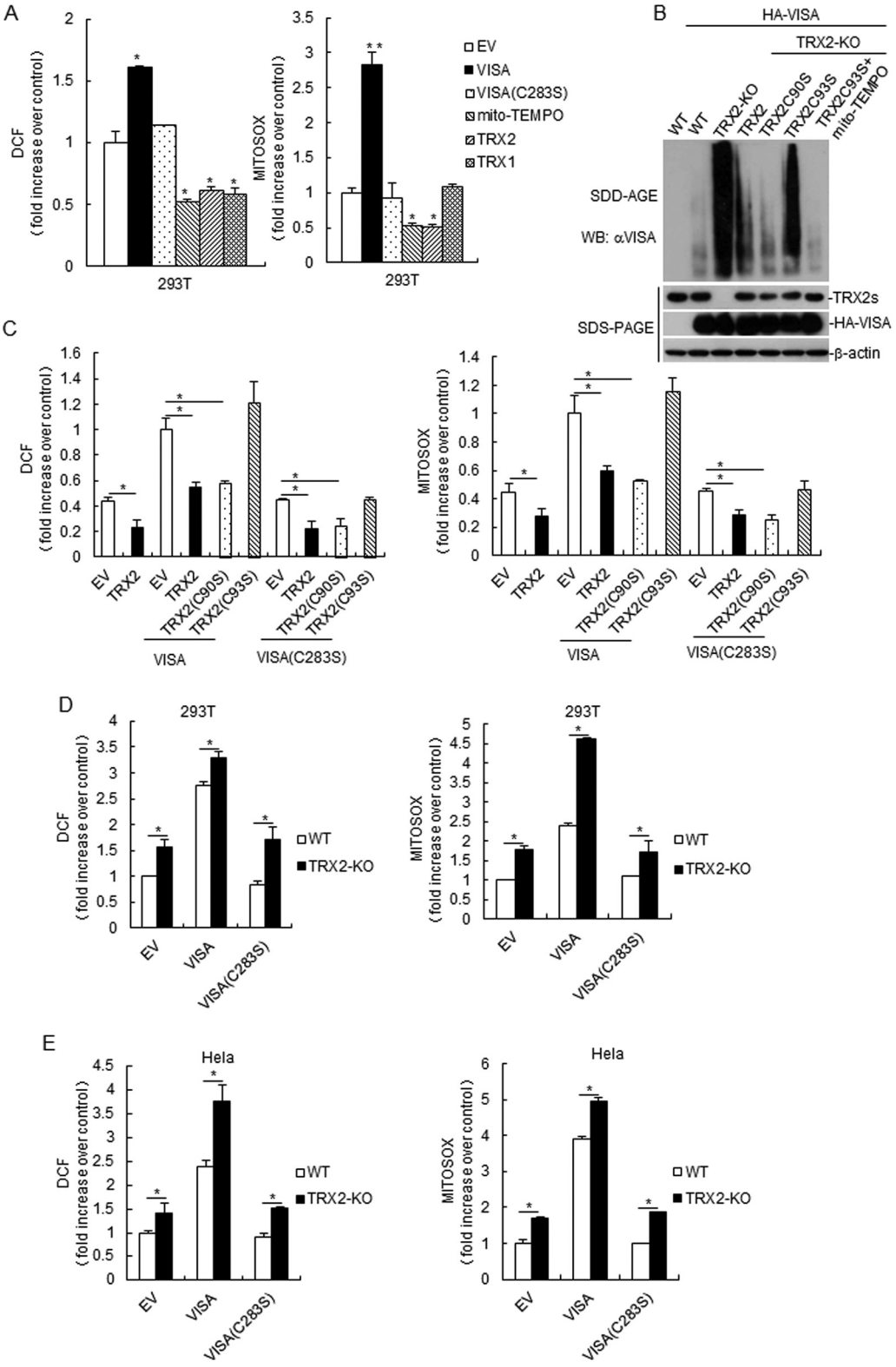

FIG 10 TRX2 mediates VISA signaling by repressing ROS production. (A) Effects of TRX2, TRX1, mito-TEMPO, or VISA or its mutant (VISAC283S) on ROS production in HEK293T cells. TRX2, TRX1, VISA, VISAC283S mutant, or empty vector were transfected into HEK293T cells for 24 h. Cells were treated with DMSO or Mito-TEMPO (250 μm) for 8 h. Cells were collected for FACS analysis to check cellular or mitochondrial ROS production by staining with DCF (left) or MitoSOX (right), respectively. Results were presented relative to the FACS mean fluorescence intensity over control cells. (B) Effects of TRX2 mutants or mito-TEMPO on VISA aggregation. Reconstitutions of TRX2 mutants in TRX2 knockout HEK293T cells were transfected with HA-VISA for 24 h after treatment or no treatment with mito-TEMPO (250 μm) for 8 h. Thereafter, crude

(Continued on next page)

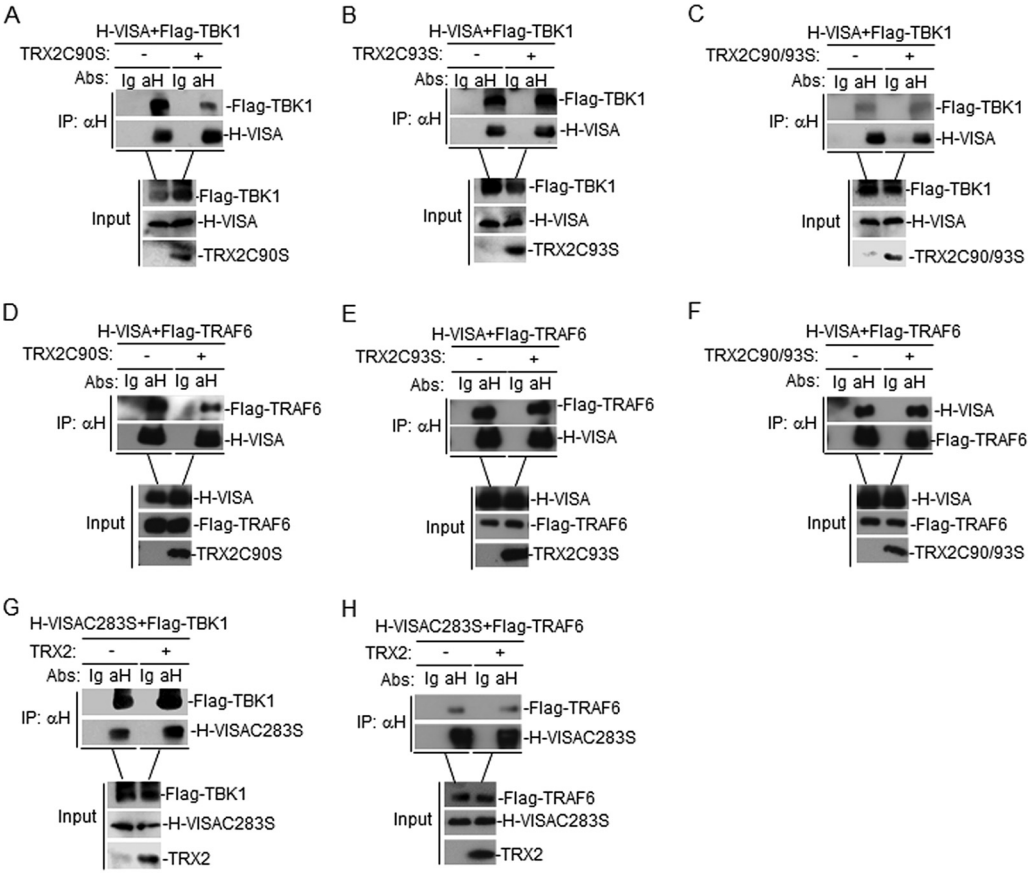

FIG 11 Effects of TRX2 or its mutants on the assembly of VISA- or its mutant-associated complex. (A to C) Effects of TRX2 mutants on VISA-TBK1 assembly. HEK293T cells (2×10^6) were transfected with the indicated plasmids (5 μg each), and then co-IP and immunoblotting were performed with the indicated antibodies. (D to F) Effects of TRX2 mutants on VISA-TRAF6 assembly. The experiments were performed as described in A. (G and H) Effects of TRX2 on VISAC283S-TBK1/TRAF6 assembly. The experiments were performed as described in A. Co-IP, coimmunoprecipitation; H, HA tag; αH, anti-HA.

RNA interference. Double-strand oligonucleotides targeting human TRX2 (number 1, 5′-GGATCTC-CTTGACAACCTTTA-3′; number 2, 5′-GGCCAAGGTGGATATTGATGA-3′; number 3, 5′-GACTTCTTCTGAG-GAGGTTCC-3′; and number 4, 5′-GATCTCCTTGACAACCTTTAA-3′) were cloned into the pSuper. Retro RNAi plasmid (Oligoengine, Seattle, WA).

RNAi-transduced HEK293T cells. HEK293T cells (1×10^6) were transfected with two packaging plasmids (10 μg of pGag-Pol and 3 μg of pVSV-G) combined with a control or TRX2-RNAi retroviral plasmid (10 μg) by the calcium phosphate precipitation method. At 12 h later, cells were incubated with antibiotic-free medium for an additional 24 h. The recombinant virus-containing medium was filtered and used to infect HEK293T cells in the presence of Polybrene (4 μg/ml). The infected HEK293T cells were selected with puromycin (0.5 μg/ml) for 14 days before conducting additional experiments.

Knockout of TRX2 HEK293T and HeLa cell lines by CRISPR-Cas9. To generate TRX2 knockout cell lines, double-stranded oligonucleotides corresponding to the target genes were cloned into the lenti-CRISPR-V2 vector and cotransfected with packaging plasmids into HEK293T cells. Thereafter, HEK293T and HeLa cells were infected with lentivirus, and infected cells were selected with puromycin (1 μg/ml) for 14 days. The following sequences were applied for targeting human TRX2 cDNA: 5′-GTGGTGTATATTGTCCGGGC-3′ (number 1) and 5′-CCCGGACAATATACACCACG-3′ (number 2).

FIG 10 Legend (Continued)
mitochondrial extracts were isolated, and then aliquots of the extracts were subjected to SDD-AGE and SDS-PAGE assays utilizing the indicated antibodies. (C) Effects of TRX2 overexpression and its mutants on ROS production in HEK293T cells induced by VISA or VISAC283S. HEK293T cells were transfected with indicated plasmids for 24 h. Cells were collected for FACS analysis to check cellular or mitochondrial ROS production by staining with DCF (left) or MitoSOX (right), respectively. Results were presented relative to the FACS mean fluorescence intensity over control cells. (D) Effects of VISA overexpression or its mutant (VISAC283S) on ROS production in TRX2-deficient HEK293T cells. The experiments were performed as described in B. (E) Effects of VISA overexpression or its mutant (VISAC283S) on ROS production in TRX2-deficient HeLa cells. The experiments were performed as described in B. Data are shown as mean ± SD of three independent experiments. ROS, reactive oxygen species; WT, wild type; EV, empty vector; KO, knockout.

TABLE 1 Primer and oligonucleotide list

Primer[a]	Sequence (5′–3′)
IFNB1-F	CAGCAATTTTCAGTGTCAGAAGCT
IFNB1-R	CAGTGACTGTACTCCTTGGCCTT
TNFα-F	GCCGCATCGCCGTCTCCTAC
TNFα-R	CCTCAGCCCCCTCTGGGGTC
IL-8-F	GAGAGTGATTGAGAGTGGACCAC
IL-8-R	CACAACCCTCTGCACCCAGTTT
IL-6-F	TTCTCCACAAGCGCCTTCGGTC
IL-6-R	TCTGTGTGGGGCGGCTACATCT
IP-10-F	GGTGAGAAGAGATGTCTGAATCC
IP-10-R	GTCCATCCTTGGAAGCACTGCA
ISG56-F	ACGGCTGCCTAATTTACAGC
ISG56-R	AGTGGCTGATATCTGGGTGC
SeV P-F	CAAAAGTGAGGGCGAAGGAGAA
SeV P-R	CGCCCAGATCCTGAGATACAGA
VSV P-F	GTGACGGACGAATGTCTCATAA
VSV P-R	TTTGACTCTCGCCTGATTGTAC
GAPDH-F	AAAATCAAGTGGGGCGATGCT
GAPDH-R	GGGCAGAGATGATGACCCTTT

[a]F, forward; R, reverse.

Cell fractionation. Cell fractionation was performed as previously described (17). Briefly, HEK293T cells (5×10^7) treated with SeV, H_2O_2, and DTT or untreated cells were washed with PBS, followed by douncing 40 times in 2-ml homogenization buffer (ApplyGen). The homogenate was centrifuged at $500 \times g$ for 10 min, and then the supernatant was centrifuged at $5000 \times g$ for another 10 min to precipitate mitochondria. The resulting supernatant was further centrifuged at $50,000 \times g$ for 30 min to obtain the cytosol fraction.

VSV plaque assay. TRX2-deficient HEK293T or HeLa cells (2×10^5) were transfected with 1 μg/ml poly(I·C) for 16 h and then infected with VSV-GFP (MOI = 0.1) for 18 h. The supernatants were diluted at $1:10^6$ and then used to infect confluent HEK293T cells for 1 h. Afterward, the supernatant was removed and overlaid with 3% methylcellulose for 3 days. Then, overlay was removed, and cells were fixed with 4% formaldehyde for 20 min and stained with 0.2% crystal violet. Plaques were counted, averaged, and multiplied by the dilution factor to determine viral titer as log10 (PFU/ml).

Statistical analysis. All data are presented as mean ± standard deviation (SD) of at least three independent experiments. A two-tailed Student's t test was applied to analyze the results, and a *P* value of <0.05 was regarded as statistically significant.

ACKNOWLEDGMENTS

We thank Hong-Bing Shu (Wuhan University) for providing plasmids and viruses.

This work was supported by grants from the Gansu Provincial Science and Technology Department of China (17JR5RA323), the National Natural Science Foundation of China (31672585 and U1501213), and the Chinese Academy of Agricultural Sciences (Y2017JC55).

We declare that we have no competing interests.

REFERENCES

1. Akira S, Uematsu S, Takeuchi O. 2006. Pathogen recognition and innate immunity. Cell 124:783–801. https://doi.org/10.1016/j.cell.2006.02.015.
2. Hiscott J. 2007. Convergence of the NF-kappaB and IRF pathways in the regulation of the innate antiviral response. Cytokine Growth Factor Rev 18:483–490. https://doi.org/10.1016/j.cytogfr.2007.06.002.
3. Durbin JE, Fernandez-Sesma A, Lee CK, Rao TD, Frey AB, Moran TM, Vukmanovic S, Garcia-Sastre A, Levy DE. 2000. Type I IFN modulates innate and specific antiviral immunity. J Immunol 164:4220–4228. https://doi.org/10.4049/jimmunol.164.8.4220.
4. Honda K, Takaoka A, Taniguchi T. 2006. Type I interferon gene induction by the interferon regulatory factor family of transcription factors. Immunity 25:349–360. https://doi.org/10.1016/j.immuni.2006.08.009.
5. Blasius AL, Beutler B. 2010. Intracellular Toll-like receptors. Immunity 32:305–315. https://doi.org/10.1016/j.immuni.2010.03.012.
6. Ishikawa H, Barber GN. 2008. STING is an endoplasmic reticulum adaptor that facilitates innate immune signalling. Nature 455:674–678. https://doi.org/10.1038/nature07317.
7. Kato H, Takeuchi O, Mikamo-Satoh E, Hirai R, Kawai T, Matsushita K, Hiiragi A, Dermody TS, Fujita T, Akira S. 2008. Length-dependent recognition of double-stranded ribonucleic acids by retinoic acid-inducible gene-I and melanoma differentiation-associated gene 5. J Exp Med 205:1601–1610. https://doi.org/10.1084/jem.20080091.
8. Yoneyama M, Fujita T. 2008. Structural mechanism of RNA recognition by the RIG-I-like receptors. Immunity 29:178–181. https://doi.org/10.1016/j.immuni.2008.07.009.
9. Xu L-G, Wang Y-Y, Han K-J, Li L-Y, Zhai Z, Shu H-B. 2005. VISA is an adapter protein required for virus-triggered IFN-beta signaling. Mol Cell 19:727–740. https://doi.org/10.1016/j.molcel.2005.08.014.
10. O'Neill LA, Bowie AG. 2010. Sensing and signaling in antiviral innate immunity. Curr Biol 20:R328–R333. https://doi.org/10.1016/j.cub.2010.01.044.
11. Zhao T, Yang L, Sun Q, Arguello M, Ballard DW, Hiscott J, Lin R. 2007. The NEMO adaptor bridges the nuclear factor-kappaB and interferon regulatory factor signaling pathways. Nat Immunol 8:592–600. https://doi.org/10.1038/ni1465.
12. Saha SK, Pietras EM, He JQ, Kang JR, Liu S-Y, Oganesyan G, Shahangian

A, Zarnegar B, Shiba TL, Wang Y, Cheng G. 2006. Regulation of antiviral responses by a direct and specific interaction between TRAF3 and Cardif. EMBO J 25:3257–3263. https://doi.org/10.1038/sj.emboj.7601220.
13. Oganesyan G, Saha SK, Guo B, He JQ, Shahangian A, Zarnegar B, Perry A, Cheng G. 2006. Critical role of TRAF3 in the Toll-like receptor-dependent and -independent antiviral response. Nature 439:208–211. https://doi.org/10.1038/nature04374.
14. Häcker H, Redecke V, Blagoev B, Kratchmarova I, Hsu LC, Wang GG, Kamps MP, Raz E, Wagner H, Hacker G, Mann M, Karin M. 2006. Specificity in Toll-like receptor signalling through distinct effector functions of TRAF3 and TRAF6. Nature 439:204–207. https://doi.org/10.1038/nature04369.
15. Spyrou G, Enmark E, Miranda-Vizuete A, Gustafsson J. 1997. Cloning and expression of a novel mammalian thioredoxin. J Biol Chem 272:2936–2941. https://doi.org/10.1074/jbc.272.5.2936.
16. Eklund H, Gleason FK, Holmgren A. 1991. Structural and functional relations among thioredoxins of different species. Proteins 11:13–28. https://doi.org/10.1002/prot.340110103.
17. Zhang R, Al-Lamki R, Bai L, Streb JW, Miano JM, Bradley J, Min W. 2004. Thioredoxin-2 inhibits mitochondria-located ASK1-mediated apoptosis in a JNK-independent manner. Circ Res 94:1483–1491. https://doi.org/10.1161/01.RES.0000130525.37646.a7.
18. Li H, Xu C, Li Q, Gao X, Sugano E, Tomita H, Yang L, Shi S. 2017. Thioredoxin 2 offers protection against mitochondrial oxidative stress in h9c2 cells and against myocardial hypertrophy induced by hyperglycemia. Int J Mol Sci 18:1958. https://doi.org/10.3390/ijms18091958.
19. Psarra A-M, Hermann S, Panayotou G, Spyrou G. 2009. Interaction of mitochondrial thioredoxin with glucocorticoid receptor and NF-kappaB modulates glucocorticoid receptor and NF-kappaB signalling in HEK-293 cells. Biochem J 422:521–531. https://doi.org/10.1042/BJ20090107.
20. Hansen JM, Zhang H, Jones DP. 2006. Mitochondrial thioredoxin-2 has a key role in determining tumor necrosis factor-alpha-induced reactive oxygen species generation, NF-kappaB activation, and apoptosis. Toxicol Sci 91:643–650. https://doi.org/10.1093/toxsci/kfj175.
21. Nonn L, Williams RR, Erickson RP, Powis G. 2003. The absence of mitochondrial thioredoxin 2 causes massive apoptosis, exencephaly, and early embryonic lethality in homozygous mice. Mol Cell Biol 23:916–922. https://doi.org/10.1128/mcb.23.3.916-922.2003.
22. Zhao Y, Sun X, Nie X, Sun L, Tang TS, Chen D, Sun Q. 2012. COX5B regulates MAVS-mediated antiviral signaling through interaction with ATG5 and repressing ROS production. PLoS Pathog 8:e1003086. https://doi.org/10.1371/journal.ppat.1003086.
23. Zhang H, Go Y-M, Jones DP. 2007. Mitochondrial thioredoxin-2/peroxiredoxin-3 system functions in parallel with mitochondrial GSH system in protection against oxidative stress. Arch Biochem Biophys 465:119–126. https://doi.org/10.1016/j.abb.2007.05.001.
24. Liu Y, Min W. 2002. Thioredoxin promotes ASK1 ubiquitination and degradation to inhibit ASK1-mediated apoptosis in a redox activity-independent manner. Circ Res 90:1259–1266. https://doi.org/10.1161/01.res.0000022160.64355.62.
25. Kawai T, Takahashi K, Sato S, Coban C, Kumar H, Kato H, Ishii KJ, Takeuchi O, Akira S. 2005. IPS-1, an adaptor triggering RIG-I- and Mda5-mediated type I interferon induction. Nat Immunol 6:981–988. https://doi.org/10.1038/ni1243.
26. Meylan E, Curran J, Hofmann K, Moradpour D, Binder M, Bartenschlager R, Tschopp J. 2005. Cardif is an adaptor protein in the RIG-I antiviral pathway and is targeted by hepatitis C virus. Nature 437:1167–1172. https://doi.org/10.1038/nature04193.
27. Seth RB, Sun L, Ea CK, Chen ZJ. 2005. Identification and characterization of MAVS, a mitochondrial antiviral signaling protein that activates NF-kappaB and IRF3. Cell 122:669–682. https://doi.org/10.1016/j.cell.2005.08.012.
28. Wang Y-Y, Liu L-J, Zhong B, Liu T-T, Li Y, Yang Y, Ran Y, Li S, Tien P, Shu H-B. 2010. WDR5 is essential for assembly of the VISA-associated signaling complex and virus-triggered IRF3 and NF-kappaB activation. Proc Natl Acad Sci U S A 107:815–820. https://doi.org/10.1073/pnas.0908967107.
29. Lei C-Q, Zhang Y, Li M, Jiang L-Q, Zhong B, Kim YH, Shu H-B. 2015. ECSIT bridges RIG-I-like receptors to VISA in signaling events of innate antiviral responses. J Innate Immun 7:153–164. https://doi.org/10.1159/000365971.
30. Zhong B, Zhang Y, Tan B, Liu T-T, Wang Y-Y, Shu H-B. 2010. The E3 ubiquitin ligase RNF5 targets virus-induced signaling adaptor for ubiquitination and degradation. J Immunol 184:6249–6255. https://doi.org/10.4049/jimmunol.0903748.
31. Nemoto Y, De Camilli P. 1999. Recruitment of an alternatively spliced form of synaptojanin 2 to mitochondria by the interaction with the PDZ domain of a mitochondrial outer membrane protein. EMBO J 18:2991–3006. https://doi.org/10.1093/emboj/18.11.2991.
32. Liu S, Chen J, Chai X, Wu J, Chen X, Wu YT, Sun L, Chen ZJ. 2013. MAVS recruits multiple ubiquitin E3 ligases to activate antiviral signaling cascades. Elife 2:e00785. https://doi.org/10.7554/eLife.00785.
33. Zeng W, Ming X, Liu S, Sun L, Chen ZJ. 2009. Key role of Ubc5 and lysine-63 polyubiquitination in viral activation of IRF3. Mol Cell 36:315–325. https://doi.org/10.1016/j.molcel.2009.09.037.
34. Nie Y, Ran Y, Zhang H-Y, Huang Z-F, Pan Z-Y, Wang S-Y, Wang Y-Y. 2017. GPATCH3 negatively regulates RLR-mediated innate antiviral responses by disrupting the assembly of VISA signalosome. PLoS Pathog 13:e1006328. https://doi.org/10.1371/journal.ppat.1006328.
35. Wang P, Yang L, Cheng G, Yang G, Xu Z, You F, Sun Q, Lin R, Fikrig E, Sutton RE. 2013. UBXN1 interferes with Rig-I-like receptor-mediated antiviral immune response by targeting MAVS. Cell Rep 3:1057–1070. https://doi.org/10.1016/j.celrep.2013.02.027.
36. Takeuchi O, Akira S. 2010. Pattern recognition receptors and inflammation. Cell 140:P805–P820. https://doi.org/10.1016/j.cell.2010.01.022.
37. Zhang P, Reichardt A, Liang H, Aliyari R, Cheng D, Wang Y, Xu F, Cheng G, Liu Y. 2012. Single amino acid substitutions confer the antiviral activity of the TRAF3 adaptor protein onto TRAF5. Sci Signal 5:ra81. https://doi.org/10.1126/scisignal.2003152.
38. Soucy-Faulkner A, Mukawera E, Fink K, Martel A, Jouan L, Nzengue Y, Lamarre D, Vande Velde C, Grandvaux N. 2010. Requirement of NOX2 and reactive oxygen species for efficient RIG-I-mediated antiviral response through regulation of MAVS expression. PLoS Pathog 6:e1000930. https://doi.org/10.1371/journal.ppat.1000930.
39. Gonzalez-Dosal R, Horan KA, Rahbek SH, Ichijo H, Chen ZJ, Mieyal JJ, Hartmann R, Paludan SR. 2011. HSV infection induces production of ROS, which potentiate signaling from pattern recognition receptors: role for S-glutathionylation of TRAF3 and 6. PLoS Pathog 7:e1002250. https://doi.org/10.1371/journal.ppat.1002250.
40. Chen L-T, Hu M-M, Xu Z-S, Liu Y, Shu H-B. 2016. MSX1 Modulates RLR-mediated innate antiviral signaling by facilitating assembly of TBK1-associated complexes. J Immunol 197:199–207. https://doi.org/10.4049/jimmunol.1600039.
41. Li Y, Chen R, Zhou Q, Xu Z, Li C, Wang S, Mao A, Zhang X, He W, Shu H-B. 2012. LSm14A is a processing body-associated sensor of viral nucleic acids that initiates cellular antiviral response in the early phase of viral infection. Proc Natl Acad Sci U S A 109:11770–11775. https://doi.org/10.1073/pnas.1203405109.
42. Zhong B, Yang Y, Li S, Wang YY, Li Y, Diao F, Lei C, He X, Zhang L, Tien P, Shu H-B. 2008. The adaptor protein MITA links virus-sensing receptors to IRF3 transcription factor activation. Immunity 29:P538–P550. https://doi.org/10.1016/j.immuni.2008.09.003.
43. Wei J, Guo W, Lian H, Yang Q, Lin H, Li S, Shu H-B. 2017. SNX8 mediates IFNgamma-triggered noncanonical signaling pathway and host defense against Listeria monocytogenes. Proc Natl Acad Sci U S A 114:13000–13005. https://doi.org/10.1073/pnas.1713462114.
44. Mao A-P, Li S, Zhong B, Li Y, Yan J, Li Q, Teng C, Shu H-B. 2010. Virus-triggered ubiquitination of TRAF3/6 by cIAP1/2 is essential for induction of interferon-beta (IFN-beta) and cellular antiviral response. J Biol Chem 285:9470–9476. https://doi.org/10.1074/jbc.M109.071043.
45. Fajian H, Lijun S, Hui Z, Brian S, Qiu-Xing J, Chen ZJ. 2011. MAVS forms functional prion-like aggregates to activate and propagate antiviral innate immune response. Cell 146:448–461. https://doi.org/10.1016/j.cell.2011.06.041.
46. Simon A, Randal H, Oliver K, Atul K, Susan L. 2009. A systematic survey identifies prions and illuminates sequence features of prionogenic proteins. Cell 137:146–158. https://doi.org/10.1016/j.cell.2009.02.044.
47. Bin L-H, Xu L-G, Shu H-B. 2003. TIRP, a novel Toll/interleukin-1 receptor (TIR) domain-containing adapter protein involved in TIR signaling. J Biol Chem 278:24526–24532. https://doi.org/10.1074/jbc.M303451200.
48. Chen D, Li X, Zhai Z, Shu H-B. 2002. A novel zinc finger protein interacts with receptor-interacting protein (RIP) and inhibits tumor necrosis factor (TNF)- and IL1-induced NF-kappa B activation. J Biol Chem 277:15985–15991. https://doi.org/10.1074/jbc.M108675200.